Master's Thesis of Ka Hyun Rhee

Detection of High Molecular Weight α-synuclein Aggregates in Human Plasma

사람 혈장에서 알파 시뉴클린 고분자 응집체의 검출

February 2022

Graduate School of Biomedical Sciences
Seoul National University
Biomedical Sciences Major

Ka Hyun Rhee

Detection of High Molecular Weight α-synuclein Aggregates in Human Plasma

Advisor Seung-Jae Lee

Submitting a master's thesis of
Science in Medicine

October 2021

Graduate School of Biomedical Sciences
Seoul National University
Biomedical Sciences Major

Ka Hyun Rhee

Confirming the master's thesis written by
Ka Hyun Rhee
January 2022

Chair	Inhee Mook (Seal)
Vice Chair	Seung-Jae Lee (Seal)
Examiner	Yong Seok Lee (Seal)

ABSTRACT

Detection of High Molecular Weight α-synuclein Aggregates in Human Plasma

Ka Hyun Rhee

Biomedical Sciences Major

Graduate School of Biomedical Sciences

Seoul National University

Parkinson's disease is a neurodegenerative disorder characterized by the accumulation of α-synuclein aggregates and selective neuronal loss of dopaminergic neurons in the substantia nigra. Fibrillar α-synuclein aggregates are a major constituent of pathological hallmarks such as Lewy bodies and Lewy neurites. These insoluble α-synuclein aggregates are known to induce neuronal dysfunction and death by interfering with various cellular pathways. Also, these aggregates are prone to transmission from cell to cell and later invade a wider area of the brain, causing the pathology to worsen over time. As α-synuclein is a key player in the development of Parkinson's disease, there were numerous attempts to identify and validate α-synuclein species as biomarkers. Although α-synuclein fibrils are essential to the pathological progress, there has been no report so far to

prove its presence in human plasma. I investigated whether α-synuclein fibrils generally exist in human plasma by making use of a refined protocol based on the previous studies. First, I showed that the new assay can be used to sufficiently reflect specific species of recombinant α-synuclein (monomer, oligomer, and fibrils). Second, I was able to measure a consistent amount of high molecular weight α-synuclein aggregates, presumably fibrils, in human plasma. In conclusion, human plasma contains α-synuclein aggregates whose sedimentation properties resemble those of fibrils, although it is difficult to definitively prove their β-sheet secondary structure or gross filamentous shape. The procedure developed in this study can be utilized in quantitative and qualitative analysis of α-synuclein fibrils in human blood and will allow us to identify new diagnostic measures for Parkinson's disease.

Keyword : Neurodegenerative disease, Parkinson's disease, α-synuclein, amyloid fibrils, human plasma, ELISA

Student Number : 2020-22060

CONTENTS

LIST OF FIGURES

RESULTS

ABBREVIATIONS

AD: Alzheimer’s disease

Aβ: amyloid-β

BBB: blood brain barrier

CSF: cerebrospinal fluid

DLB: Dementia with Lewy bodies

ELISA: enzyme-linked immunosorbent assay

FA: formic acid

PBS: phosphate based saline

PBS-T: phosphate based saline-Tween

PD: Parkinson’s disease

PMCA: protein misfolding cyclic amplification

RT QuIC: real-time quaking-induced conversion

RT: room temperature

SDS: sodium dodecyl sulfate

SDS – PAGE: sodium dodecyl sulfate – polyacrylamide gel electrophoresis

TEM: transmission electron microscopy

ThT: Thioflavin-T

α-syn: α-synuclein

INTRODUCTION

1. Parkinson's disease : clinical features and α –synuclein

PD is the second most common neurodegenerative disorder that affects 2 − 3% of the population older than 65 years of age [1], [2]. PD patients develop cardinal motor symptoms, as well as various non-motor symptoms, including disruptions in sleep–wake cycle regulation, cognitive impairment, alterations in mood and affect, autonomic dysfunction, and sensory deficits (most commonly hyposmia) [3]. Based on the widely accepted criteria set by the International Parkinson and Movement Disorder Society (MDS), core features of bradykinesia, rigidity, and resting tremor are essential for a clinical diagnosis of PD [4]. For a clinical diagnosis of PD at the highest level of certainty, additional evidence such as L-DOPA responsiveness and the absence of red flags (eg., rapid progression of gait impairment within 5 years after onset) are required [4].

Accuracy of a clinical diagnosis of PD is only slightly above 80% even with the application of the strictest diagnostic criteria, and the current gold standard for diagnosis is the post-mortem pathological examination [5]. Neuropathological features of PD include loss of dopaminergic neurons in the substantia nigra [6] and the abnormal deposition of α-syn in the form of Lewy pathology [7]. Lewy pathology includes Lewy bodies, which are round eosinophilic inclusions in neuronal perikarya, and Lewy neurites, which are axonal inclusions [8]. Since amyloid fibrils formed by cross β-sheet conformations of α-syn compose the majority of these Lewy pathologies, immunohistochemistry for α-syn is applied for

detection of these pathologies for post-mortem analysis [9]. Neuronal loss and Lewy pathology are two major pathological features that are both required for a conclusive diagnosis of idiopathic PD.

There were studies that identified missense mutations, duplications, and triplications in SNCA (the gene encoding α-syn) that cause familial PD and single-nucleotide polymorphisms in SNCA that increase the risk for sporadic PD [10], [11], [12]. Also, studies showed that overexpression of α-syn in transgenic animal models induce neuropathological inclusions, neuronal loss, and motor symptoms recapitulating the pathological and clinical features of PD [13]. These pieces of evidence strongly support the concept that α-syn is a key player in the pathogenesis of PD.

2. Physiological function and structure of α –synuclein

α-syn is mainly localized in presynaptic terminals, although it is also found in cell bodies, nuclei, and axons of neurons [14]. The physiological function of α-syn is not fully understood, but there have been reports of it modulating soluble N-ethylmaleimide-sensitive factor (NSF) attachment protein receptor (SNARE) complex assembly at the nerve terminal, thereby contributing to the regulation of exocytosis or neurotransmitter release [15], [16]. Accumulation of α-syn results in abnormal redistribution of the SNARE proteins [17], and α-syn has been shown to protect against progressive neurodegeneration in mice deficient in cysteine-string protein-α (CSPα), strongly implicating the important function of α-syn in SNARE complex assembly under conditions of stress. [18].

α-syn is a natively unfolded 14 kDa protein composed of three distinct regions: the amino terminus (residues 1-95), non-amyloid-β component (NAC) (residues 61-95), and carboxyl terminus (residues 96-140) [19]. The amphipathic lysine-rich amino terminus holds an essential role in regulating its interactions with lipid membranes, and a disordered carboxyl-terminus has been implicated in interactions with metals [20]–[22]. The central region of α-syn, namely the NAC region, contains a highly hydrophobic motif that is crucial for α-syn aggregation; the deletion of segments within the NAC region significantly suppresses α-syn oligomerization and fibrillation in vitro and in cell-based assays [23], [24].

3. Pathological post-translational modifications and aggregation of α–synuclein

1) Phosphorylated α-syn

The most studied post-translational modification of α-syn is phosphorylation, given that phosphorylation at Ser129 is identified in 90% of aggregated α-syn in Lewy bodies of the brains from PD patients, whereas only 4% or less is identified in brains of healthy subjects [25], [26]. Apart from S129, there were attempts to elucidate the effect of phosphorylation at other sites such as Ser87 and Tyr125 [27]. Although phosphorylation of α-syn has been widely studied, there are conflicting results as to whether phosphorylation promotes or prevents aggregation and neurotoxicity [27], [28].

2) Nitrated α-syn

Oxidative stress has been implicated in the pathogenesis of PD. It was shown that α-syn is nitrated in the major filamentous blocks and in the insoluble fractions of affected brain regions of synucleinopathy patients [29]. The action of oxygen and nitric oxide leads to the nitration of four tyrosine residues (Y39, Y125, Y133, and Y136) in α-syn [30].

Hodara et al. demonstrated that monomeric and dimeric forms of nitrated α-syn speed the fibril formation and seed the fibrillation of non-modified α-syn, whereas nitrated α-syn oligomers inhibit the fibril formation [31].

3) Truncated α-syn

Besides full-length α-syn, there exist small amounts of truncated species with molecular masses of 10–15 kDa in the Lewy bodies [32]. It is estimated that truncated α-syn accounts for 15% of α-syn in Lewy bodies [33]. Five subtypes were detected using mass spectrometry and present C-terminal truncations ending at D-115 (α-syn-D115), D-119 (α-syn-D119), N-122 (α-syn-N122), Y-133 (α-syn-Y133) and D135 (α-syn-D135) [32]. Previous studies showed that some truncated forms of α-syn may also occur under normal conditions, but brain extracts from PD and DLB patients contain significantly higher amounts of truncated α-syn in SDS- and urea-soluble fractions compared to healthy controls [38], [39]. In addition, several studies on the kinetics of the C-terminal truncated α-syn revealed that they aggregate more readily and could act as effective seeds to accelerate the aggregation of full-length α-syn [34], [36].

4) Oligomeric and fibrillar α-syn

α-syn acquires neurotoxic properties during an aggregation process in which soluble α-syn monomers (14 kDa) initially form oligomers (28 kDa – 1 MDa), then progressively merge to form large, insoluble α-syn fibrils (> 2 MDa) [37]. Insoluble α-syn fibrils can be identified based on three main characteristics. First, they have an unbranched filamentous structure when visualized by TEM or atomic force microscopy. Second, cross-β sheet conformation can be detected with circular dichroism spectroscopy [38]. Third, they show dye binding capacity with chemicals such as Congo red and ThT [39], [40]. Compared to fibrils, monomers are natively unstructured. Oligomers are α-syn multimers that do not possess the three features of fibrils.

α-syn aggregates including oligomers and fibrils have been associated with the pathogenesis of PD. The fibrillar forms of α-syn are detected primarily in Lewy bodies, which localize in cell bodies [7], [41]. In the case of oligomeric α-syn, numerous studies proved their existence in vivo under pathological conditions. SDS-resistant, low- and high-molecular-weight oligomers have been detected in the brains of PD patients [42] and in brains of transgenic animal models of synucleinopathy [43]. The effects of these aggregates in the pathogenesis of PD will be discussed later in the next section.

As mentioned earlier, post-translational modifications, including oxidative stress and truncation of α-syn are implied to induce aggregation of α-syn to oligomeric forms [33], [44]. Under in vitro conditions, oligomeric α-syn that are rich in β-sheets can be formed by increasing α-syn concentrations and shaking at 37 °C [45], adding metal ions (e.g., Fe^{2+} and Cu^{2+}) [46], imposing oxidative stress [47], or adding various ligands, such as dopamine [48]. The generated oligomers vary in

stability, morphology, and toxicity; some are on-fibrillar pathway species while others are off-fibrillar pathway oligomers [49], [50].

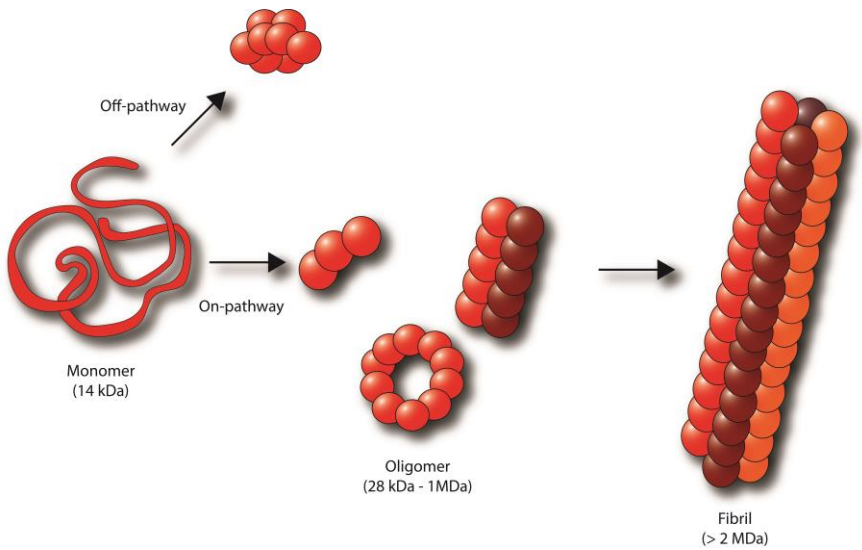

Figure 1. On-pathway and off-pathway aggregation of α-syn

4. Pathological role of aggregated α–synuclein in PD

α-syn fibrils are known to exert neurotoxicity by modifying the function of cytosolic organelles such as the endoplasmic reticulum, the Golgi, the mitochondria, and the lysosomes [51], by altering cellular proteostasis [52], and by triggering neurodegeneration by activating microglia and causing chronic neuroinflammation [53]. Also, α-syn fibrils seed the conversion of soluble α-syn into higher molecular weight aggregates [54], thereby inducing cell to cell propagation of these fibrils and driving the spread of pathology to wider areas of the brain [55].

The toxicity of oligomeric aggregates are most studied in locations such as the

axons and presynaptic terminals, where they are reported to induce synaptosomal dysfunction [56], [57]. Also, small spherical oligomers (2–6 nm) are reported to exert toxic effects by promoting neuronal degeneration and aberrant calcium currents in cultured primary cortical neurons [58]. Whether fibrils or oligomers are more neurotoxic is still controversial because of the difficulty in comparing the proteins with different sizes and shapes, but only fibrils have the ability to seed further fibrillation and thus contribute to the propagation of pathology to neighboring areas [50].

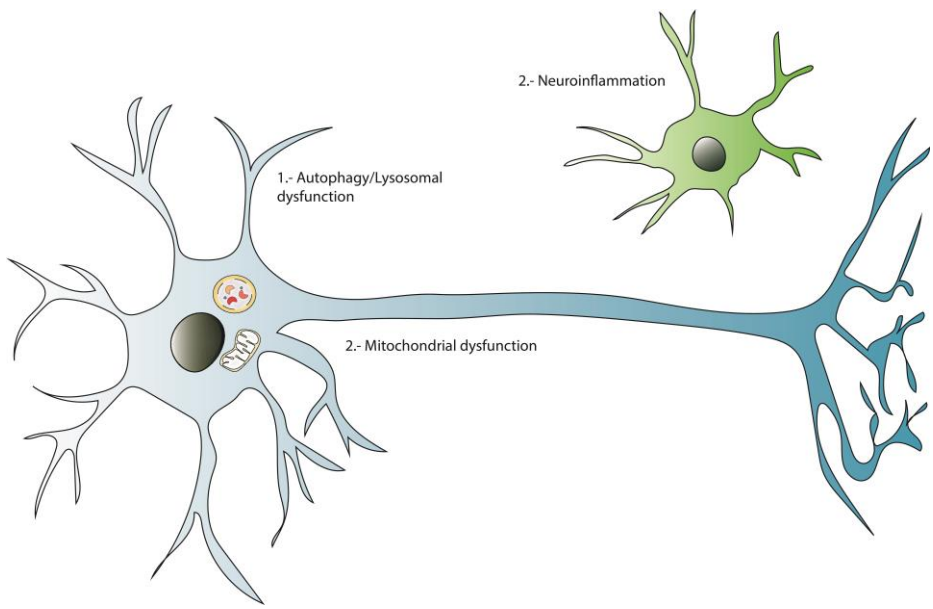

Figure 2. Pathological role of *α*-syn fibrils in neurons

5. Biomarkers and methods for diagnosis of Parkinson's disease

PD is currently an intractable disease due to the limitations of inaccurate diagnosis and symptomatic treatment. Therefore, applicable biomarkers are required to enhance diagnostic confidence in early disease and to screen PD in its pre-symptomatic stages. Since the current treatment available acts by merely making up for the loss in dopamine, it cannot alter the progress of the disease [10]. Early diagnosis of potential patients in their prodromal stages can help to tackle and prevent the loss of neurons before irreversible changes occur.

Aggregation of α-syn is key to the pathological process in the development of PD [2]. Various species of α-syn (total, phosphorylated, aggregated) were the most studied and promising, among a pool of potential biomarkers including lysosomal enzymes, neurofilament light chain, and classic AD biomarkers [59], [60]. There were numerous attempts to detect and compare levels of α-syn in blood and CSF for diagnosis or predictive screening of PD. Total and aggregate α-syn levels in the CSF showed a concordant trend in between studies, but the diagnostic accuracy was not enough to be applied to clinical context. In the case of human plasma, there were conflicting or statistically nonsignificant results regarding changes in total and aggregate α-syn levels [61]–[63]. Since α-syn can be measured in the ng or pg scale, sensitive methods such as ELISA, electrochemiluminescence, xMAP techonology(Luminex), and immunomagnetic reduction were applied for these studies.

While obtaining and preparing samples such as plasma and CSF, it is important to

confirm the absence of hemolysis. Red blood cells hold 99% of total α-syn with less than 1% of the total detected in the plasma, platelets and peripheral blood mononuclear cells, which means that hemolysis of several red blood cells can strongly influence the measurement of α-syn [64].

Recently, new methods such as PMCA and RT-QuIC on CSF yielded the highest sensitivity (95%) and specificity (100%) in distinguishing neuropathologically diagnosed PD patients [65], [66]. However, lumbar puncture is too invasive a procedure for routine diagnosis, and the task remains to extend these results to more easily accessible tissue such as blood plasma.

	Plasma/Serum	Red blood cells	CSF
Total α-synuclein	=	=	↓
Phosphorylated α-synuclein	↑	↑	↑
Aggregated α-synuclein	↑	↑	↑
NfL	=	N/A	=
Lysosomal enzymes activities	N/A	N/A	↓
Aβ42, Total tau	N/A	N/A	↓, =

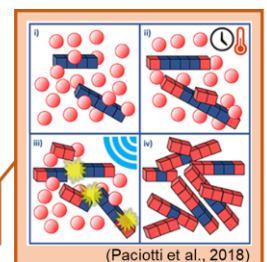

(Paciotti et al., 2018)

Protein misfolding cyclic amplification & Real-time quaking-induced conversion: highest sensitivity (95%) and specificity (100%)

Figure 3. Biomarkers and methods for diagnosis of PD

A table based on the paper by *Parnetti et al.* [60]

6. Purpose of this study

Currently, there is no accurate and applicable blood-based diagnostic method for PD. Previous studies pointed to accumulation of α-syn fibrils in the brain as a prerequisite for the development of PD, and thus α-syn aggregates were one of the

major targets for development of diagnostic methods. Moreover, recent findings showed that the conformation of fibrils from brain extracts can be differentiated among distinct synucleinopathies such as multiple systemic atrophy and PD through comparing the levels of phosphorylation, the binding propensity to specific antibodies, and protonation levels [67], [68]. I hypothesized that α-syn fibrils exist in human plasma, with the idea that their presence could lead to quantitative or qualitative measures of diagnosis. The purpose of this study was to establish a new method to detect and quantify α-syn fibrils in human plasma. Based on the recent paper demonstrating successful and simple separation of α-syn species (monomers, oligomers, and fibrils) [69], I refined the protocol to 'an ultracentrifugation based ELISA assay' for application to human plasma. I first validated its usage by testing it on in vitro α-syn species. Afterwards, I applied the assay to human plasma derived from three donors to yield consistent measurements of large aggregates.

This study is important because it is the first evidence of the presence of aggregates heavy enough to settle down upon ultracentrifugation in human plasma. Considering the fact that currently, the most promising method for PD diagnosis is the amplification of fibril seeds in body fluids, demonstration of the presence of large α-syn aggregates in human plasma should be of high significance.

MATERIALS AND METHODS

1. Protein Purification

There were minor adjustments to the protocol by Fauvet et al. [70] BL21 (DE3) (RBC Korea, Seoul, Korea, RH217) cells were transformed with human wild type α-syn expressing pDdulGC vector, then grown on a kanamycin agar plate overnight. The next day, a single colony was inoculated to 100 ml of LB medium with 50 μg/ml kanamycin (Amresco) and incubated overnight at 30 ℃. The following day, the pre-culture was transferred at a ratio of 1 : 200 to 2.4 liter of LB with kanamycin. When the OD_{600} of the culture reached between 0.6 and 0.7, 0.1 mM isopropyl β-D-1-thiogalactopyranoside (Beamsbio) was added for induction, followed by incubation for 3 hours. Cells were harvested by centrifugation at 4000 g for 15 min at 4 ℃. Lysis was performed on ice, by resuspending the cell pellet in 20 mM Tris, pH 8.0 containing protease inhibitor cocktail (Sigma-Aldrich, P8465), and ultrasonicated (Vibracell VCX130, Sonics, Newtown, CT) at 6W applied in 30-s pulses followed by a 30-s pause, for a total time of 5 min. After centrifugation at 13,999 rpm in an A50-8 rotor (Hanil, Supra R22) for 20 min at 4 ℃, the supernatant was retrieved and heated at 100 ℃ in boiling water for 10 min. Denatured and precipitated proteins were removed in a second centrifugation step (A50-8 rotor, 13999 rpm, 4 ℃, 20 min). The supernatant was filtered through 0.22 μm membranes and applied at 1 ml/min to a HiTrap Q FF anion exchange chromatography column (GE healthcare Life Sciences). Elution was done at 3

ml/min by applying a gradient of concentrations up to 1.0 M NaCl over 15 column volumes in a basis of 20 mM Tris, pH 8.0. α-syn eluted at 300 ~ 370 mM NaCl. α-syn eluted fractions (as determined by SDS-PAGE and Coomassie blue analysis) were then combined and purified a second round by size exclusion chromatography using a Hiload 16/600 Superdex 200 pg column (GE Healthcare Life Sciences) equilibrated with 50 mM Tris, pH 7.5, 150 mM NaCl. Proteins were eluted at 1 ml/min with the same equilibration buffer; pure fractions were pooled and dialyzed overnight against deionized water at 4 °C using a 10-kDa cutoff dialysis membrane. α-syn was then flash-frozen and lyophilized.

2. SDS–PAGE Analysis

Samples for SDS-PAGE were mixed in 1 × Laemmli sample buffer (62.5 mM Tris, pH 6.8, 10% glycerol, 2% SDS, 2.5% β-mercaptoethanol, 0.025% bromophenol blue) and loaded onto 12 % polyacrylamide gels. The gel was run at 150 V for 1 hr 20 min in running buffer (25 mM Tris, 192 mM Glycine, 0.1% SDS, pH 8.3), followed by staining with Imperial™ Protein Stain (Thermo Fisher) and destaining with distilled water.

3. Preparation of Fibrils

For fibrillation, recombinant α-syn was primarily filtered through a 100-kDa membrane (Pall, OD100C34) and incubated (330 μM in Dulbecco's PBS) at 37 °C

for 5 days with constant shaking at 1,050 rpm in a ThermoMixer C (Eppendorf, Hamburg, Germany, 5382000015). In all the methods to be mentioned, the concentration of α-syn samples such as monomers, oligomers, and fibrils were measured using BCA assay (Thermo Fisher Scientific, 23225).

The degree of β-sheet formation was tracked every day with ThT fluorescence. Recombinant α-syn samples were mixed with 50 μL of 10 μM ThT (Sigma, T3516) solution in glycine – NaOH (pH 8.5). After incubation in the dark for 5 min, fluorescence was measured at 450 nm excitation wavelength and 490 nm emission wavelength on a Synergy NEO plate reader (Biotek, Winooski, VT, USA).

4. Preparation of Oligomers and Monomers

Oligomers were prepared as described in the previous papers [45], [71]. Lyophilized α-syn monomers were dissolved to 12 mg/ml in Dulbecco's PBS, filtered through a 0.22 μm membrane (Pall, ODM02C34) and incubated in a ThermoMixer C (Eppendorf) at 37 °C at 900 rpm for 5 h. Large aggregates were removed by centrifugation for 10 min at 12000 g. The supernatant was applied to a Superdex 200 Increase 10/300 GL (GE Healthcare Life Sciences) and eluted with PBS buffer at a 0.5 ml/min flow rate. Oligomer fractions distinguished by UV peak were pooled and stored at 4 °C. All further experiments involving use of oligomers were performed in 5 days after the formation of oligomers.

For preparation of pure monomers, recombinant monomers were dissolved in Dulbecco's PBS, and filtered through a 100-kDa membrane (Pall, OD100C34). It was shown from the previous study [69] that a 100-kDa cut off is sufficient to

separate monomers from other multimers.

5. Transmission Electron Microscopy

0.1 – 0.4 mg/ml of protein was adsorbed onto 200-mesh carbon-coated copper grids (Electron Microscopy Sciences, Hatfield, PA, USA, CF200-Cu). In the case of fibrils, 10 μl of 2% uranyl acetate (Electron Microscopy Sciences, #22400) was additionally dropped for negative staining. The prepared grids were observed using a JEM1010 transmission electron microscope (JEOL, Akishima, Tokyo, Japan). The length or diameters of protein were measured with Image J software (U. S. National Institutes of Health, Bethesda, Maryland, USA).

6. Western Blotting

Western blotting was performed as previously described [72]. Samples were not boiled in Laemmli sample buffer prior to loading unless mentioned otherwise. For primary antibody, anti-α-syn antibody (syn211, Abcam, ab80627, 1:1000) was used. The membrane was detected with ECL solution (GE Healthcare, RPN2232). Image obtainment was done using an Amersham Imager 600 (GE Healthcare) and for analysis, Multi Gauge (v.3.0) software (Fujifilm, Akishima, Tokyo, Japan) was used.

7. Combined Centrifugation and ELISA Protocol

This protocol was newly devised based on the previous findings of Lashuel et al. [69] and can be applied for the quantification of separate α-syn species of monomers, oligomers or fibrils in a biological sample.

This protocol consists of two steps : (1) a centrifugation step for the isolation of fibrils from soluble species (2) two ELISA systems that detect either total α-syn or only aggregates.

1. Blood plasma was first thawed in 37 °C, and all the subsequent experiments were done in RT to prevent the formation of insoluble cryoprecipitate. Promptly after thawing, 1% of Protease inhibitor cocktail (Sigma Aldrich, P8340) and 1% Triton-X was added.

   In the case of recombinant protein, measured amounts of monomers, oligomers, and fibrils were prepared as a mixture.
2. A total sample volume of 500 ~ 1000 μL went through ultracentrifugation at 100,000 g for 30 min at 22 °C. Since fibrils are more prone to dissociation at cold temperatures [73], experiments were done at RT.
3. After centrifugation, retrieval of the supernatant, the soluble species, was carried out. The isolated pellets were resuspended in ELISA sample dilution buffer.
4. The supernatant and resuspended pellet were both measured with total and aggregate α-syn ELISAs. In a recombinant protein experiment context

[69], the pellets were previously demonstrated to be fibrils which were heavy enough to settle down upon ultracentrifugation.

This newly devised protocol can be utilized for quantification of separate species of α-syn in biological samples, especially those samples with high density, without fear of loss during filtration or other preparation steps.

8. ELISA

ELISA was performed as previously mentioned [74]. Ninety-six-well ELISA plates (Maxisorp; Nunc, Rochester, NY) were coated with 1 μg/ml capture antibody in 50 mM carbonate buffer (pH 9.6) overnight at 4 °C. Plates were washed 5 times in PBS with 0.05% Tween 20 (PBS-T) in between steps. SuperBlock T20 PBS blocking buffer (Pierce) was loaded for 1 h at RT with modest shaking. While blocking, standards were freshly prepared with serial dilutions of recombinant α-syn monomers or fibrils. The samples and standards were incubated at RT for 2.5 h followed by 1 μg/ml biotinylated reporter antibody in blocking buffer being added and incubated at RT for 1.5 h. Subsequently, avidin-conjugated peroxidase (ExtrAvidin; Sigma) was added at a 1:1500 dilution in blocking buffer for 1 h at RT. For the substrate reaction, 100μL of 3,3,5,5-tetramethylbenzidine solution (Sigma) was added to each well and incubated until right before saturation. The reaction was stopped with 50 μL of 2 N H_2SO_4 and the absorbance was measured at 450 nm with a Synergy NEO plate reader (Biotek, Winooski, VT, USA).

For total α-syn ELISA, capture antibody of Syn-1 (BD Transduction Laboratories, 610787) and detection antibody of biotinylated 274 (ABL Bio) was used. For

aggregate α-syn ELISA, capture antibody of either 274 or 3A9 (ABL Bio) was paired with detection antibody, biotinylated 274. 274 and 3A9 antibodies were both provided by ABL bio (South Korea).

9. Human Plasma

Under the Institutional Review Board's review exemption approval (IRB no. E-2102-100-1197) from Seoul National University and Red Cross Review Board approval, I received 3 packs of citrated (CPDA-1) plasma, each from a separate anonymous female donor in her twenties. The pack was thawed at 37°C and was aliquoted into 2 ml Eppendorf tubes. The aliquots of plasma were kept frozen at −20 °C until use.

10. Dissociation of Fibrils with Formic Acid

Pellet prepared from human plasma as described before in this method section was first resuspended in 10 volumes of formic acid (pH 2). Subsequently, the pellet was neutralized with 7.1 volumes of Tris (pH 11). These neutralized samples were directly loaded to ELISA plates.

11. Statistical Analysis

Values shown in the graphs are presented as Mean ± S.E.M. The graphs were drawn with Prism 7 software (GraphPad Software Inc., San Diego, CA, USA).

RESULTS

Purification of α-synuclein

Protein purification of α-syn was performed similar to the previous study [70]. Since α-syn is intrinsically unfolded, lysate from transformed E. coli first went through a boiling step in order to clear out other proteins. Afterwards, the boiled lysate proceeded to subsequent steps of anion exchange chromatography and size exclusion chromatography.

During anion exchange chromatography, α-syn eluted at 25 ~ 35 mS/cm of conductivity (Figure 1A). Fractions 13 ~ 16 were pooled and loaded to the next round of size exclusion chromatography (Figure 1B). A major peak of α-syn formed at volumes corresponding to 30 ~ 40 kDa in size (Figure 1C). Subsequently, fractions 31 ~ 33 were pooled, lyophilized and stored for further experiment. The final product held a purity over 98%, determined by Coomassie staining (Figure 1D).

Characterization of α-synuclein Fibrils and Oligomers

The formation of fibrils from purified α-syn monomers was assessed with ThT fluorometry. The sigmoidal curve reached an equilibrium phase at 75 hours after start of incubation (Figure 2A). On the fifth day, elongated α-syn fibrils with a diameter of 10–15 nm were observable with TEM (Figure 2A).

In order to evaluate whether quantification of separate α-syn species of monomers, oligomers, and fibrils was feasible with a combined ultracentrifugation and ELISA

assay, I first needed to apply the assay to an in vitro mixture of protein. The mixture of protein was prepared with pure portions of each of the three quantified species. Pure monomers and fibrils were each prepared with 100-kDa filtration and 100,000 g ultracentrifugation. To prepare pure oligomers, a high concentration of α-syn monomers was incubated for 5 hours, subsequently followed by separation with a Superdex 200 10/300 GL column [45], [69]. As shown in the total chromatogram (Figure 2B), oligomeric α-syn eluted at fractions 18 and 19, shortly after the void volume, in concordance to the previous studies [45], [49], [69]. The amount of protein measured with 280 nm UV absorbance indicated a 1.2 % of the whole transitioned to oligomers. Western blot results confirmed that the UV absorbance precisely reflected the amount of α-syn protein (Figure 2C). Fractions 29 ~ 32 comprised the high chromatography peak of monomers. Longer exposure of western blots with the fractions eluted before the monomer peak showed that oligomers of fractions 18 and 19 barely migrate into the gel as previously mentioned in another study [45] (Figure 2D). These oligomers were temporarily resistant to SDS and heat, but were no longer visible after 24 hours or a single freeze-thaw cycle.

TEM images were obtained from fractions 18 and 19 (Figure 2E,F). The earlier eluted fraction contained ovoid aggregates with an average maximum Feret diameter of 32.6 nm (Figure 2F,G). Fraction 19 was composed of round α-syn aggregates with a smaller, less varied diameter with an average of 21.9 nm (Figure 2F,G). Although some studies reported α-syn oligomers with beta sheet structures [75], my oligomers yielded minimal ThT fluorescence signal compared to fibrils (Figure 2H).

Separation and Quantification of Recombinant α-synuclein Monomers, Oligomers, and Fibrils

I refined a protocol from the previous paper [69] to devise an assay that would be more compatible to highly dense biological samples. Instead of using a 100-kDa filter to divide oligomers and monomers, the mixture went through a single round of ultracentrifugation (Figure 3A). Afterwards, the supernatant and the pellet were measured with both total α-syn ELISA and aggregate α-syn ELISA. Two aggregate ELISA systems were used in this study, "274 – 274" and "3A9 – 274". In the case of the "274 – 274" system, the specificity of the system to detect aggregates was achieved through the mechanism in which a multimer is required for it to bind to both capture and detector antibodies that recognize an identical epitope. For the "3A9 – 274" system, the 3A9 antibody itself is already aggregate specific, being raised against fibrils formed from c-terminal truncated α-syn (previously characterized in yet unpublished data from Minsun Choi et al.). Both of these systems specifically detected α-syn aggregates and did not recognize up to 800 ng/ml of monomers (Figure 3C,4B).

Total and aggregate α-syn ELISA measurements of the pellet most probably indicated the amount of fibrils as shown in a previous study [69]. aggregate α-syn ELISA results of the supernatant reflected the amount of oligomers. Also, the value of aggregate α-syn ELISA subtracted from total α-syn ELISA in the supernatant roughly reflected the amount of monomers.

Pure α-syn monomers, oligomers, and fibrils were mixed at a ratio of 10 : 1 : 10 based on measurements with BCA. Portions from each step were imaged with

TEM (Figure 3B). Monomers were not visible due to small molecular size. No elongated rods were detected in the supernatant, indicating that fibrils do not remain in the supernatant after ultracentrifugation. The reconstituted pellet contained shorter fragments of fibrils, compared to the starting material (Figure 3C). Also, the ELISA results after ultracentrifugation showed that 60 ~ 70% of the starting fibril amount was measurable, indicating dissociation of fibrils. 143% of the original oligomers were measured as aggregates in the supernatant (Figure 3D). These phenomena may have resulted from rapid shifts to an unpredictable thermodynamic equilibrium. Furthermore, a mere 30 minutes on ice is sufficient to change much of the conformation of fibrils [73]; when preparing the mixture, ice cold monomer and oligomer solutions were inevitably mixed to fibrils due to different storing conditions. The proteins' instability and dynamic change may have accounted for discrepancies between measured concentrations before and after the procedure. Overall, quantification with this assay fairly reflected the presence and amount of each of the species.

Detection of High Molecular Weight α-synuclein Aggregates in Human Plasma

The aforementioned assay was tested on human plasma from three anonymous female donors in their twenties. Citrated human plasma was obtained from the Red Cross following review exemption approval of the Institutional Review Board. Total α-syn measured from the three samples were 100 ~ 250 ng/ml (Figure 4A). All three pellets had detectable signals from total and aggregate ELISA assays (Figure 4A,C), implying that high molecular weight aggregates, presumably fibrils,

do exist in human plasma. In the supernatant, up to 2 ng/ml of small aggregates were detected. All of these aggregates were not detectable before ultracentrifugation, possibly due to the blocking capacity of other high concentration proteins in blood plasma (60 ~ 80 mg/ml measured in BCA). To confirm that various contents of blood plasma deterred the full measurement of fibrils, a known amount of recombinant α-syn fibrils was added to plasma and subsequently measured with aggregate ELISA. Only 4 ~ 8 % of the added amount was detectable (Figure 4D), indicating that the majority of α-syn fibrils were masked from measurement and that a process to separate aggregate species into a less dense environment is necessary. Another unexpected result was the high variability of measurements in pellet among repeated trials on each donor sample. To test whether the variance could be reduced with increased solubility and dissociation, a further experiment with the use of formic acid was undertaken.

Concordant Levels of α-synuclein in the Pellet of Plasma Between Donors After Dissociation with Formic Acid

Taking into account methods from the previous studies [76], [77], applying formic acid to dissociate and accurately measure Aβ in dense plaques, I determined a condition (2.26% formic acid, pH 2) in which α-syn fibrils were completely dissociated to monomers. Using the procedure described in Figure 3A, the pellet was resuspended in formic acid (pH 2), then neutralized with Tris (pH 11) buffer. This pellet was measured with both total and aggregate α-syn ELISAs. For the total ELISA, two standard curves were plotted. The standard based on PBS-T yielded a higher signal compared to the other with monomers that were first added

with formic acid then neutralized with Tris buffer (Figure 4A). Measurements of the neutralized pellet derived from human plasma was based on the FA + Tris curve. Surprisingly, there was minimal variance within each individual and among the individuals (Figure 4B). Also, the increase in measurement (41.6 ng/ml mean from all values) compared to without formic acid dissociation indicated that highly packed fibrils were dissociated to a higher number of singular molecules, monomers, with epitopes recognized by antibodies. For aggregate ELISA, similarly, two standard curves were plotted. The standard based on PBS-T yielded a higher signal compared to the other with fibrils that were serially diluted in neutralization buffer (Figure 4C). Measurements of the neutralized pellet derived from human plasma was based on the standard "Neutralization Buffer" curve. Minimal amount to zero aggregates were detected in all samples, indicating that the pellet was indeed dissociated fully to monomers (Figure 4D). The overall scheme for detecting high molecular weight α-syn aggregates is presented in Figure 4E.

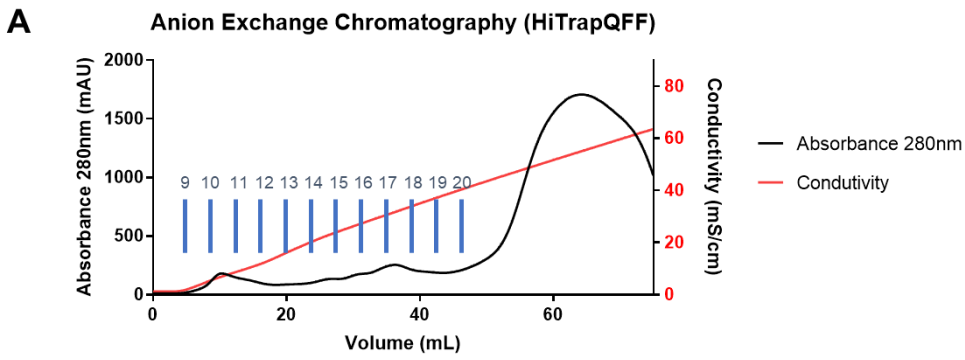
A
Anion Exchange Chromatography (HiTrapQFF)
Absorbance 280nm (mAU)
Conductivity (mS/cm)
Volume (mL)
9 10 11 12 13 14 15 16 17 18 19 20
Absorbance 280nm
Condutivity

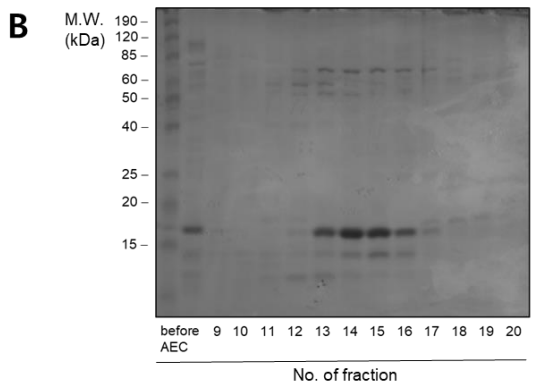
B
M.W. (kDa)
190
120
85
60
50
40
25
20
15
before AEC
9 10 11 12 13 14 15 16 17 18 19 20
No. of fraction

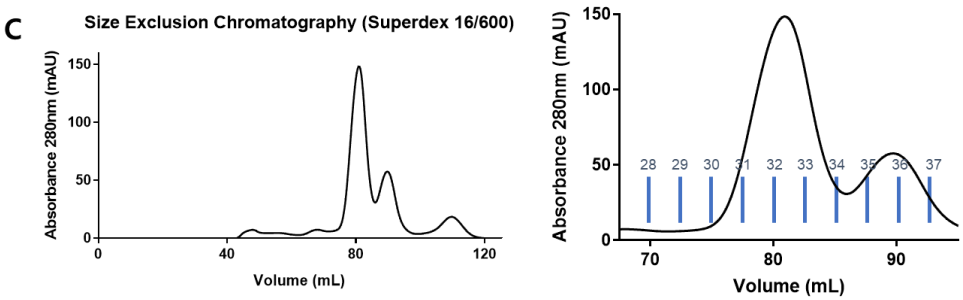
C
Size Exclusion Chromatography (Superdex 16/600)
Absorbance 280nm (mAU)
Volume (mL)
28 29 30 31 32 33 34 35 36 37

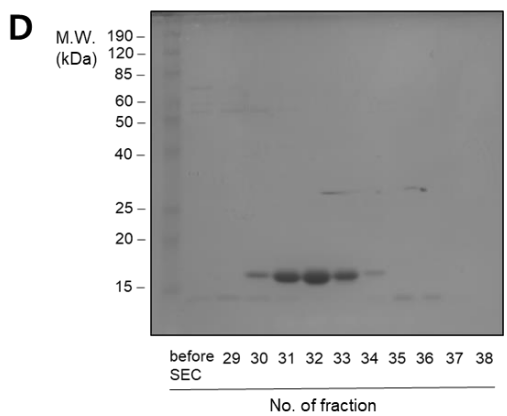
D
M.W. (kDa)
190
120
85
60
50
40
25
20
15
before SEC
29 30 31 32 33 34 35 36 37 38
No. of fraction

Figure 1. Purification of α-synuclein.

(A) Anion exchange chromatography results from supernatant obtained after boiling and centrifugation. The blue rods indicate the beginning of each eluted fraction. (B) The corresponding fractions from figure (A) were analyzed with SDS-PAGE and coomassie staining. Compared to before the step of anion exchange chromatography, fractions 13 – 16 showed higher purity and concentration of α-syn. (C) These fractions 13 – 16 were pooled and injected for size exclusion chromatography. The UV peak near 80 ml of elution volume is magnified in the right. The blue rods likewise set the start of each eluted fraction. (D) The eluted fractions were analyzed with SDS-PAGE and Coomassie staining. Fractions 31 – 33 yielded high purity of α-syn, and thus were pooled for subsequent dialysis and lyophilization.

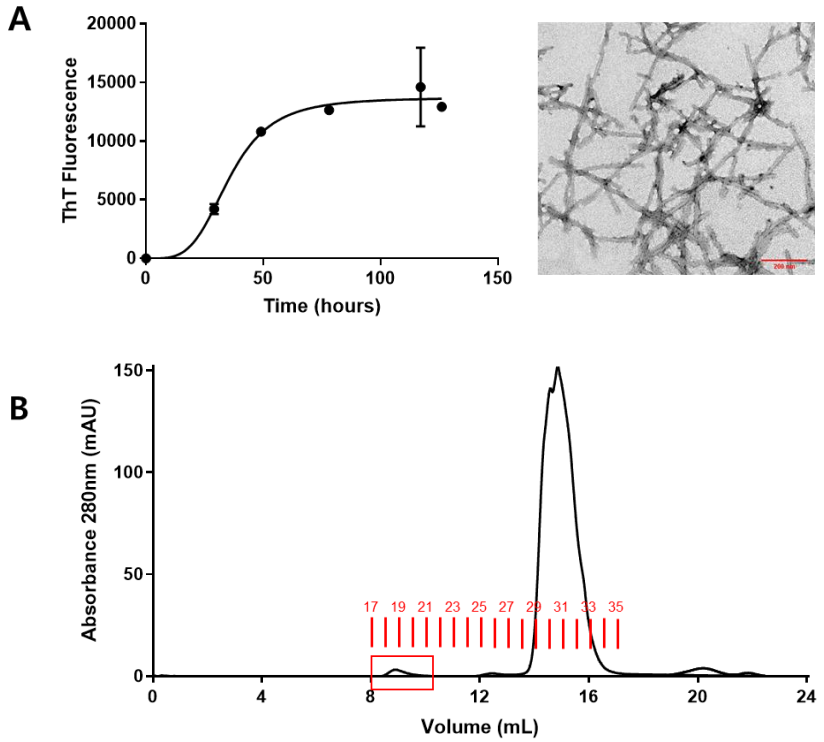
A
ThT Fluorescence
20000
15000
10000
5000
0
0
50
100
150
Time (hours)
B
Absorbance 280nm (mAU)
150
100
50
0
17 19 21 23 25 27 29 31 33 35
0
4
8
12
16
20
24
Volume (mL)

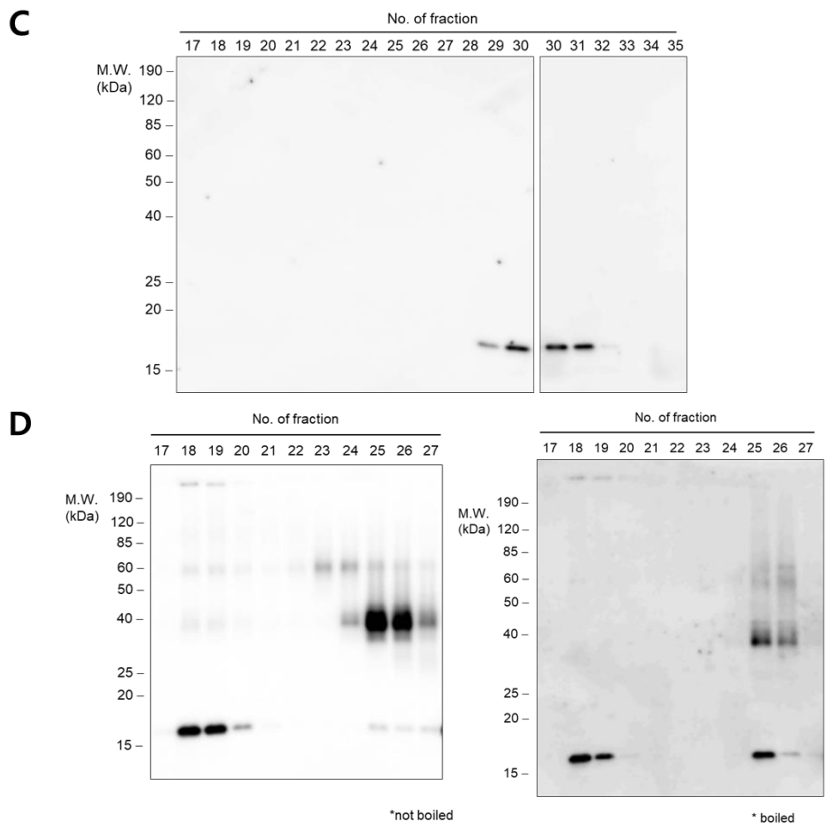
C
No. of fraction
17 18 19 20 21 22 23 24 25 26 27 28 29 30 30 31 32 33 34 35
M.W. (kDa)
190
120
85
60
50
40
25
20
15
D
No. of fraction
17 18 19 20 21 22 23 24 25 26 27
M.W. (kDa)
190
120
85
60
50
40
25
20
15
*not boiled
No. of fraction
17 18 19 20 21 22 23 24 25 26 27
M.W. (kDa)
190
120
85
60
50
40
25
20
15
* boiled

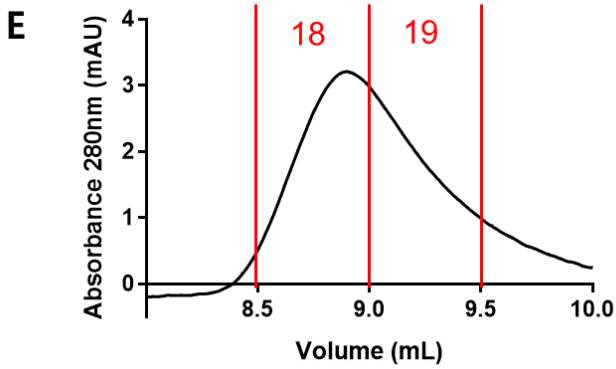
E
18
19
Absorbance 280nm (mAU)
0
1
2
3
4
8.5
9.0
9.5
10.0
Volume (mL)

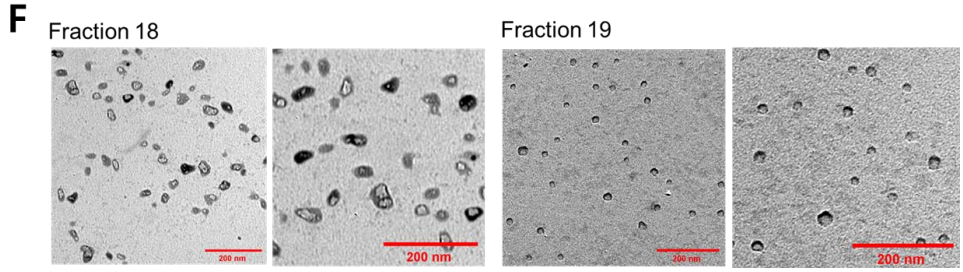
F
Fraction 18
Fraction 19
200 nm
200 nm
200 nm
200 nm

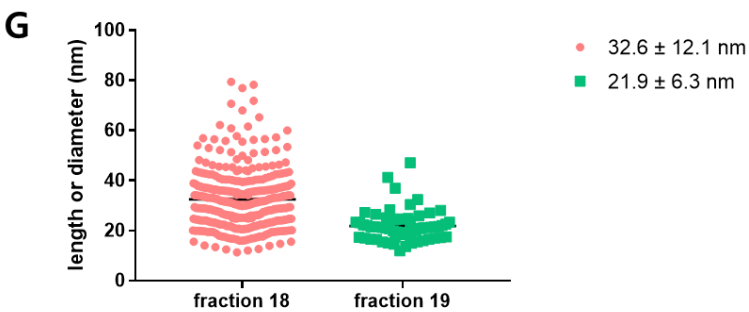
G
length or diameter (nm)
0
20
40
60
80
100
fraction 18
fraction 19
32.6 ± 12.1 nm
21.9 ± 6.3 nm

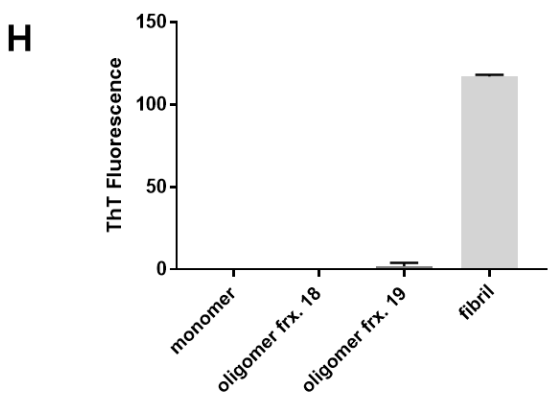
H
ThT Fluorescence
0
50
100
150
monomer
oligomer frx. 18
oligomer frx. 19
fibril

Figure 2. Preparation and characterization of α-synuclein fibrils and oligomers

(A) Fibrillation of α-syn monomers measured with ThT fluorescence for 5 consecutive days. To the right is a representative TEM image of the fibrils on day 5. The red scale bar indicates 200 nm in length. (B) Size exclusion chromatography (Superdex 200 Increase 10/300 GL column) results of α-syn monomers after 5 hours of incubation at 12 mg/ml. The red rods indicate the beginning of each fraction, and is analyzed with several western blots (C), (D). (C) Western blot of fractions spanning from fractions 17 – 35. Samples were not boiled, and antibody Syn211 was used as primary antibody. (D) To visualize the oligomers in detail, fractions 17 – 27 were loaded for western blot. Antibody Syn211 was used as primary antibody. To the left, samples were not boiled in Laemmli sample buffer. To the right, they were boiled. (E) A magnified image of the red box in figure 2(B). Elution volumes of 8.5 − 9.5 ml contained fractions 18 and 19, the oligomer fractions. (F) TEM images of fractions 18 and 19 without negative staining. All the red scale bars indicate a length of 200 nm. (G) The length or diameter of oligomers from image (F) were measured with Image J and presented as mean ± S.E.M. Fraction 18 oligomers had an average diameter of 32.6 nm while fraction 19 oligomers held an average of 21.9 nm. (H) ThT fluorescence was measured for each of the species. 40μL of 5μg/ml of protein was incubated with ThT.

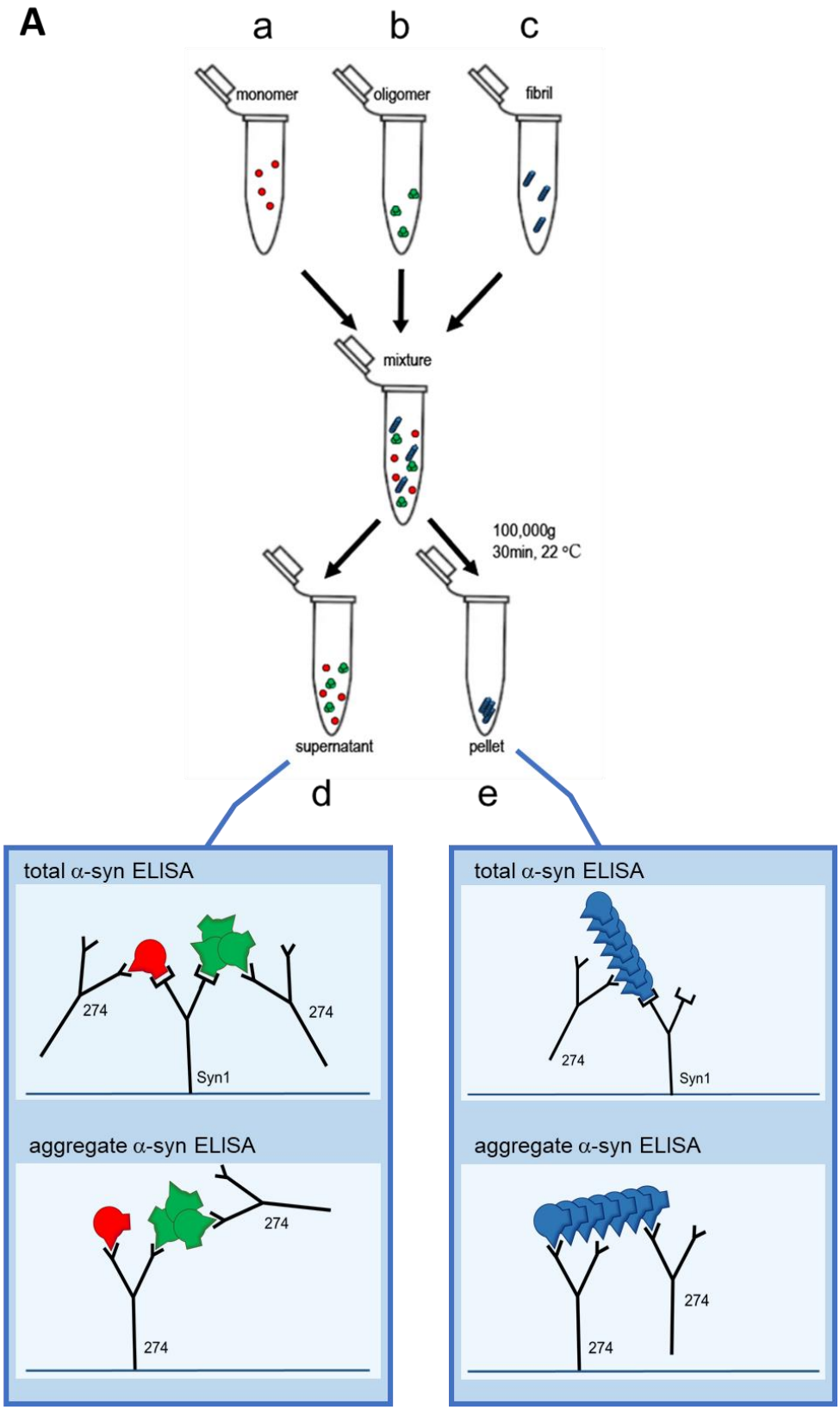
A
a
b
c
monomer
oligomer
fibril
mixture
100,000g
30min, 22 °C
supernatant
pellet
d
e
total α-syn ELISA
274
274
Syn1
aggregate α-syn ELISA
274
274
total α-syn ELISA
274
Syn1
aggregate α-syn ELISA
274
274

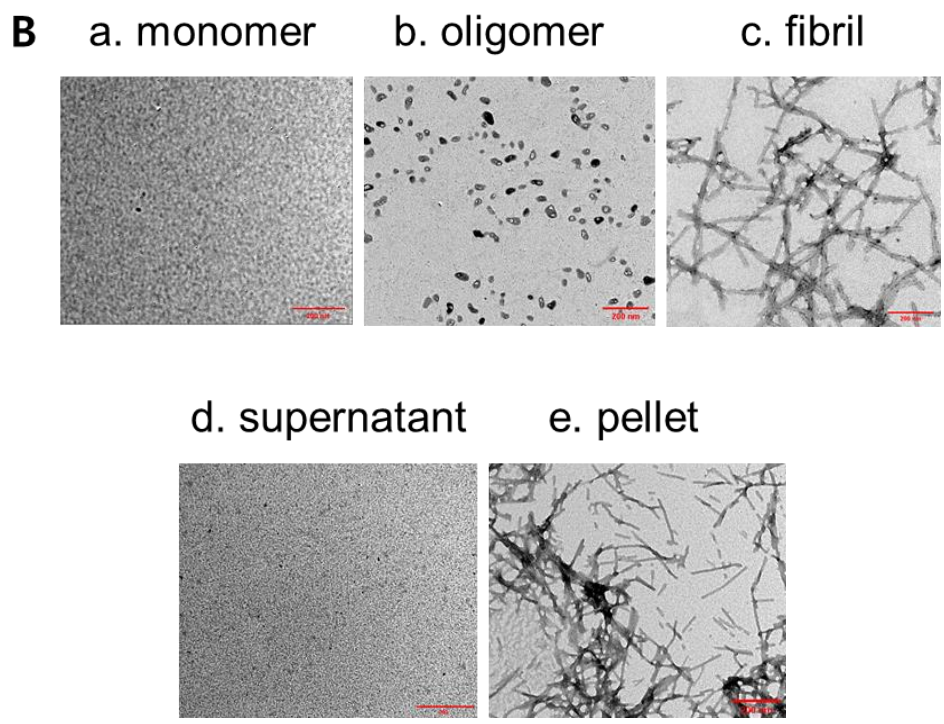
B
a. monomer
b. oligomer
c. fibril
d. supernatant
e. pellet
C
aggregate α-syn ELISA
(274-274)
Absorbance (450nm)
2.5
2.0
1.5
1.0
0.5
0.0
-0.5
20
40
50
400
800
α-synuclein dose (ng/mL)
Aggregate
Monomer
D
total α-syn
α-synuclein (μg)
50
40
30
20
10
0
mono
oligo
fib
sup.
pellet
α-syn aggregates
(274-274)
α-synuclein (μg)
40
30
20
10
0
mono
oligo
fib
sup.
pellet
*starting amount per 240uL

Figure 3. Ultracentrifugation paired with ELISA to separate and quantify recombinant α-synuclein monomers, oligomers, and fibrils

(A) A schematic illustration of the separation and quantification of α-syn species. (B) TEM images of recombinant α-syn samples a – e from scheme (A). Only c and e went through an additional step of negative staining with 2% uranyl acetate. (C) Standard curve of α-syn aggregate ELISA with a coating antibody of 274 and detector antibody of biotinylated 274. A linear curve formed with fibrils as standards, but no signal was detectable up to 800 ng/ml of monomers. (D) Recombinant α-syn samples throughout procedure (A) were measured with total and aggregate α-syn ELISAs. For total α-syn ELISA, a coating antibody of Syn1 and a detector antibody of biotinylated 274 was used. Aggregate α-syn ELISA was done at conditions mentioned in (C).

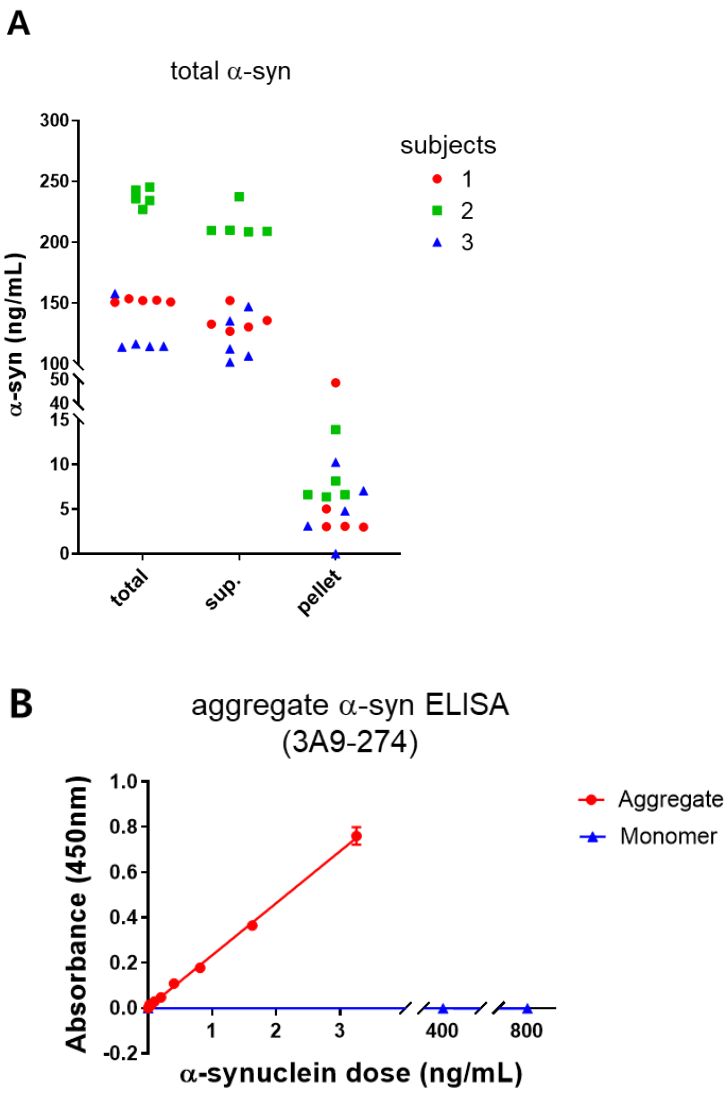
A
total α-syn
subjects
1
2
3
α-syn (ng/mL)
300
250
200
150
100
50
40
15
10
5
0
total
sup.
pellet
B
aggregate α-syn ELISA
(3A9-274)
Aggregate
Monomer
Absorbance (450nm)
1.0
0.8
0.6
0.4
0.2
0.0
-0.2
1
2
3
400
800
α-synuclein dose (ng/mL)

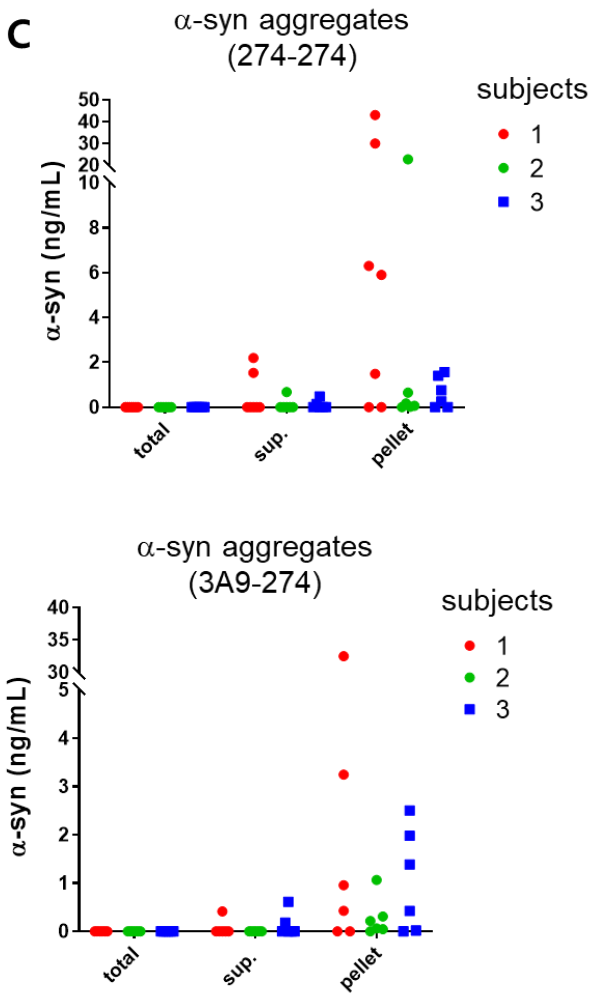
C
α-syn aggregates
(274-274)
subjects
1
2
3
α-syn (ng/mL)
50
40
30
20
10
8
6
4
2
0
total
sup.
pellet
α-syn aggregates
(3A9-274)
subjects
1
2
3
α-syn (ng/mL)
40
35
30
5
4
3
2
1
0
total
sup.
pellet

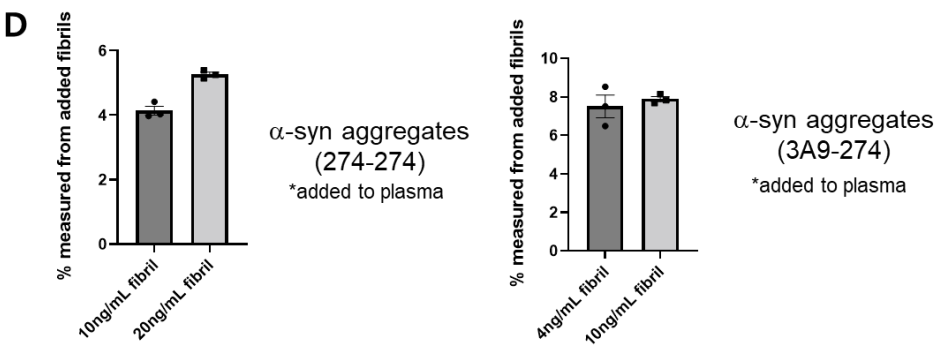
D
% measured from added fibrils
6
4
2
0
10ng/mL fibril
20ng/mL fibril
α-syn aggregates
(274-274)
*added to plasma
% measured from added fibrils
10
8
6
4
2
0
4ng/mL fibril
10ng/mL fibril
α-syn aggregates
(3A9-274)
*added to plasma

Figure 4. Detection of high molecular weight α-synuclein aggregates in human plasma

(A) Total α-syn ELISA measurements of human plasma before and after ultracentrifugation. 1 - 3 indicate anonymous donors with a randomly given number. Each experiment was repeated 5 times. (B) Standard curve of α-syn aggregate ELISA with a coating antibody of 3A9 and detector antibody of biotinylated 274. A linear curve formed with fibrils as standards, but no signal was detected up to 800 ng/ml of monomers. (C) α-syn aggregate ELISA to measure in human plasma before and after ultracentrifugation. For the 274 - 274 system, the experiment was repeated 7, 6, and 6 times for each donor plasma. As for the 3A9 - 274 system, each experiment was repeated 6 times. (D) A known amount of recombinant fibrils (4 ng/ml, 10 ng/ml, and 20 ng/ml) were added to plasma from donor number 1 and subsequently measured with aggregate α-syn ELISA. Both 274 – 274 system (left) and 3A9 - 274 system (right) were used.

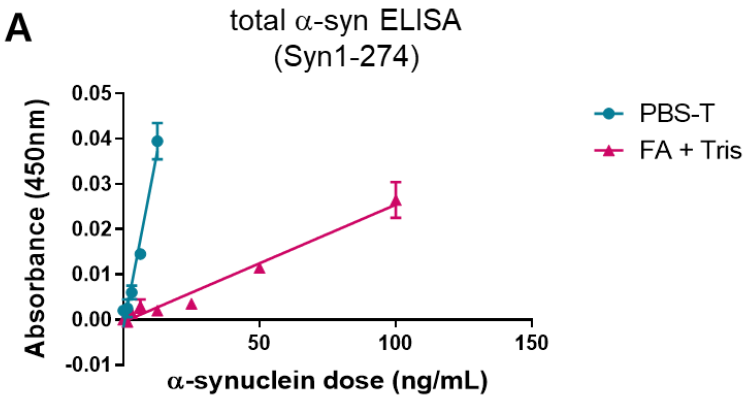
A
total α-syn ELISA
(Syn1-274)
Absorbance (450nm)
0.05
0.04
0.03
0.02
0.01
0.00
-0.01
50
100
150
α-synuclein dose (ng/mL)
PBS-T
FA + Tris

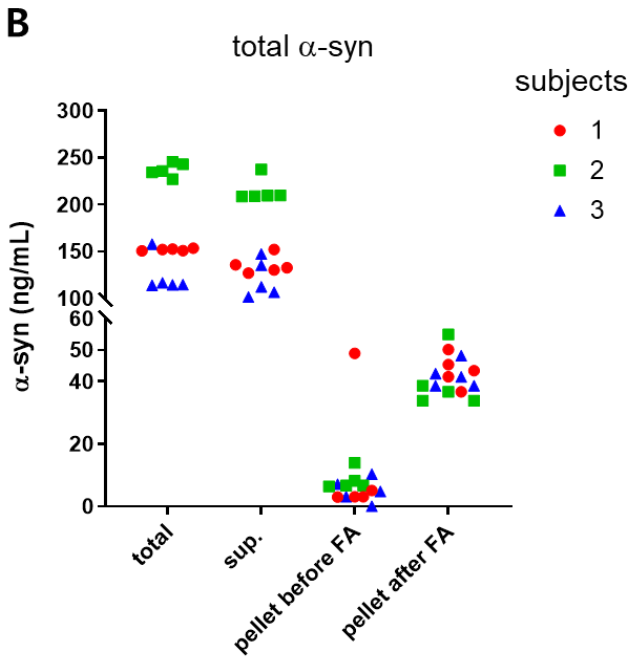
B
total α-syn
subjects
1
2
3
α-syn (ng/mL)
300
250
200
150
100
60
50
40
20
0
total
sup.
pellet before FA
pellet after FA

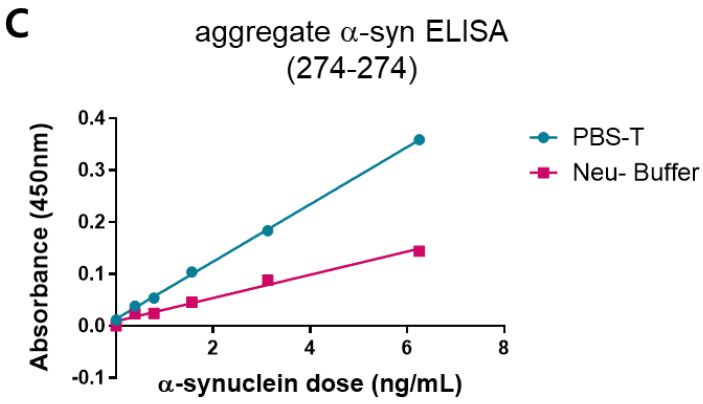
C
aggregate α-syn ELISA
(274-274)
Absorbance (450nm)
0.4
0.3
0.2
0.1
0.0
-0.1
2
4
6
8
α-synuclein dose (ng/mL)
PBS-T
Neu- Buffer

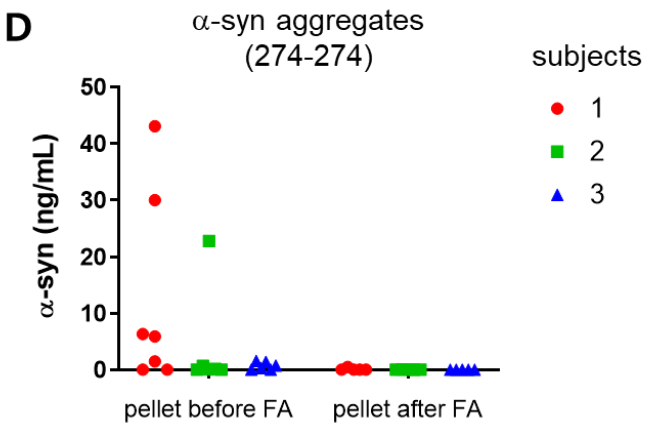
D
α-syn aggregates
(274-274)
subjects
1
2
3
α-syn (ng/mL)
50
40
30
20
10
0
pellet before FA
pellet after FA

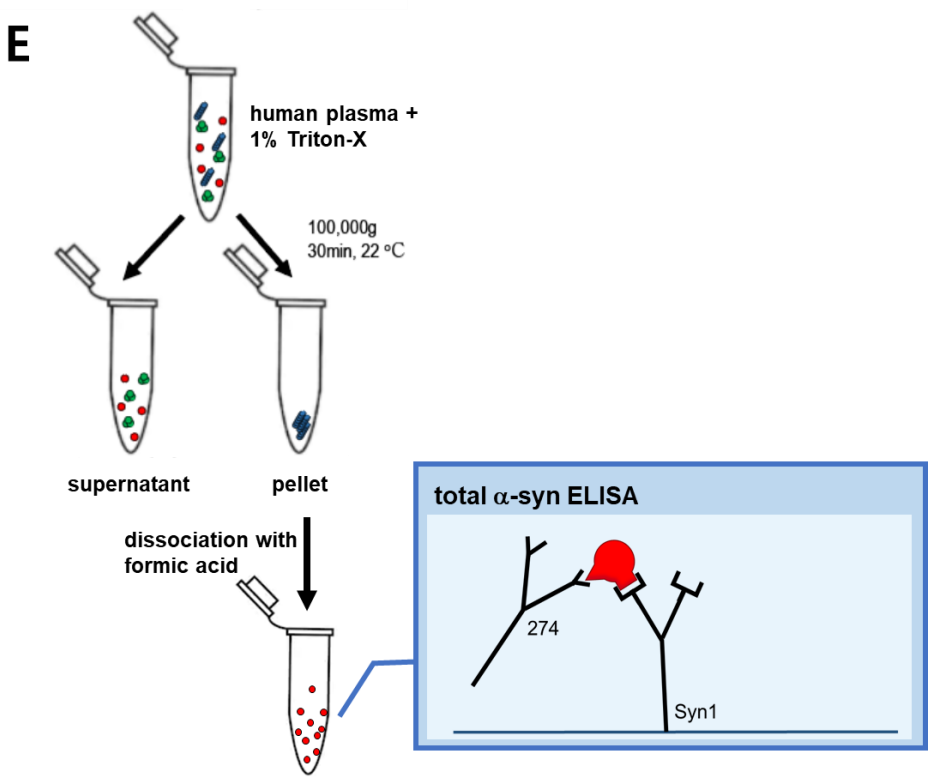
E
human plasma +
1% Triton-X
100,000g
30min, 22 °C
supernatant
pellet
dissociation with
formic acid
total α-syn ELISA
274
Syn1

Figure 5. Consistent measurements of α-synuclein in pellet of plasma after dissociation with formic acid

(A) Standard curve of total α-syn ELISA with a coating antibody of Syn1 and detector antibody of biotinylated 274. The blue dots represent points derived from standard ELISA buffer, PBS with tween. The purple dots represent points derived from monomers that are primarily dissolved with fomic acid (pH 2) then neutralized to pH 7.4 with Tris buffer. (B) Total α-syn ELISA measurements of the pellet, which were derived from human plasma after ultracentrifugation and dissociated with formic acid (pH 2) then neutralized. Measurements were based on the 'formic acid + Tris' standard curve. 1 - 3 indicate anonymous donors with a randomly given number. Each experiment was repeated 5 times. (C) Standard curve of α-syn aggregate ELISA with a coating antibody of 274 and detector antibody of biotinylated 274. The blue dots represent points derived from standard ELISA buffer, PBS with tween. The purple dots represent points derived from fibrils that are diluted in already neutralized buffer of formic acid and Tris. (D) α-syn aggregate ELISA measurements of the pellet, which were derived from human plasma after ultracentrifugation and dissociated with formic acid (pH 2) then neutralized. Measurements were based on the 'Neutralized Buffer' standard curve. Each experiment was repeated 5 times. (E) Scheme for detecting high molecular weight α-syn aggregates in human plasma.

DISCUSSION

In this study, I investigated whether I could detect and measure α-syn fibrils in human plasma, by refining the method from a recent study [69]. I began with preparing pure portions of separate recombinant α-syn species, monomers, oligomers, and fibrils. These species were generated only with shaking without any treatment of chemicals. In the case of oligomers, the characteristics were in line with previous papers [45], [69]. Next, by applying a combined ultracentrifugation and ELISA protocol, I was able to distinguish and separately measure the amount of each species in a mixture, as proven by TEM images of each sample. In blood plasma, I showed that ultracentrifugation makes it possible to detect large aggregates, which originally cannot be detected at all without the process. The masking effect (Figure 4D) may have been caused by high concentrations of other proteins in plasma that interfere with α-syn in binding to antibodies. One unexpected result was the high variation among multiple repetitions with the same donor derived pellet upon resuspension with PBS-T. This could have been due to the fact that hydrophobic fibrils are prone to binding to the walls of tubes or pipette tips. Another explanation could be that the variability in dissociation is difficult to control during resuspension. In order to address these two issues, formic acid was added for complete dissociation of pellet to monomers. Surprisingly, increasing solubility with dissociation resulted in consistent, reproducible measurements. In conclusion, it was difficult to measure in human plasma the high molecular weight aggregates as itself with this assay, but after the insoluble aggregates were dissociated, consistent quantification was possible.

This is the first study in my knowledge to show that large aggregates, presumably fibrils, exist in human plasma. Aggregation of α-syn into elongated amyloids is in the center of the pathological development process of PD [78], [79], [80] and thus has long since been the target for biomarker development [59], [60]. In previous studies, it may had been difficult to measure α-syn fibrils in biological samples or the brain of healthy subjects due to the absence of sensitive detection methods specific for fibrils and the relative scarceness of α-syn compared to other abundant proteins. My results of the existence of fibrils in plasma not only add new knowledge but can lead to new opportunities in diagnostic research. Fibrils in plasma may be compared between PD patients and the healthy subjects with both quantitative and qualitative approaches. For example, structural analysis with fluorescent dyes or hydrogen deuterium exchange measurements can be done to distinguish between healthy states and several dementia causing diseases [67], [68]. Moreover, my results show the potential applicability of PMCA and RT-QuIC trials on human plasma, because there is a high probability of the presence of fibrils that can act as seeds. Since the very first introduction of the PMCA method 20 years ago [81], there has been no follow up study on the application of this technique to human plasma. As covered in this study, handling blood plasma encompasses some tricky conditions arising from high protein concentrations of the samples, and appropriate pre-processing of samples may be needed to optimize for amplification. This study has some limitations. First, the assay could not yield consistent aggregate measurements from human plasma, especially in the pellet fraction. Only after full dissociation could the large aggregates be measured reproducibly. My approach to indirectly measure aggregates is somewhat similar to that of a previous paper which showed that the level of increase in detection levels after full

monomerization of plasma Aβ has diagnostic value in AD [82]. Testing on less concentrated biofluids, such as CSF, may provide insights into whether this issue is caused by characteristics confined to blood plasma. Second, since minute amounts of aggregates were present in the pellet, it was difficult to directly prove that the pellets contained elongated fibrils, with general methods such as circular dichroism, electron microscopy, or dye binding assays. There is a possibility that elongated rods could be visible in the pellet through atomic force microscopy, but it will still be difficult to specify whether they are precisely α-syn fibrils. Third, simplifying the steps for quantification is required for this assay to be tested on a larger cohort. An approach similar to the Multimer Detection System-Oligomeric Aβ (MDS-OAβ) developed by PeopleBio Inc. can be applied for detection of α-syn fibrils [83]. Through incubating human plasma with recombinant α-syn, endogenous fibrils could be amplified and measured more readily without an additional ultracentrifugation step.

This study raises questions and calls for follow up studies. Further comparison between measurements in PD patients and healthy subjects are needed to determine diagnostic value of this assay. Also, where the large aggregates in blood are originated and whether a blood to brain propagation of pathology occurs are important questions to be pursued. The mechanism related to the potential diagnostic value of measuring plasma α-syn in patients is still unclear. α-syn is expressed in neurons, gut endocrine cells, red blood cells, and platelets [15], [64], [84], but it is yet unknown which source accounts for the majority of α-syn in human plasma. There have been studies showing that brain derived exosomes in the blood contain α-syn [85], [86], but the reliability of the L1CAM markers to

specifically detect neuron-derived extracellular vesicles is controversial [87]. As for the blood to brain propagation, there is no previous report of its contribution to the pathogenesis of PD. However, blood to brain transmission of α-syn was proved to occur in spite of the BBB, and was accelerated after LPS induced disruption of the BBB [88]. Also, there is a study that showed an increase in induced nitric oxide synthase, a pro-inflammatory factor, in the brain of mice after intravenous injection of the exosomes originated from PD patient-derived RBCs [89]. Thus, further application of this proposed assay to patients and understanding the origins and functions of the plasma α-syn are interesting topics for future studies.

CONCLUSION

In this study, I devised an assay to quantify separate species of α-syn (monomers, oligomers, and fibrils) and applied it to detect high molecular weight α-syn aggregates in human plasma. First, the reliability of the assay was verified with recombinant protein. Subsequently, using the assay, α-syn aggregates that resemble the sedimentation properties of fibrils were detected in human plasma. The use of formic acid to fully dissociate these aggregates proved to be an additional step essential for the accurate measurement in human plasma. In brief, this study shows possibility of new diagnostic approaches by applying the analytical tools developed in this study to the quantification of the aggregates in plasma of PD patients.

Reference

[1] T. Pringsheim, N. Jette, A. Frolkis, and T. D. L. Steeves, “The prevalence of Parkinson’s disease: A systematic review and meta-analysis,” *Movement Disorders*, vol. 29, no. 13, pp. 1583–1590, 2014, doi: 10.1002/mds.25945.

[2] L. Hirsch, N. Jette, A. Frolkis, T. Steeves, and T. Pringsheim, “The Incidence of Parkinson’s Disease: A Systematic Review and Meta-Analysis,” *NED*, vol. 46, no. 4, pp. 292–300, 2016, doi: 10.1159/000445751.

[3] K. R. Chaudhuri and A. H. Schapira, “Non-motor symptoms of Parkinson’s disease: dopaminergic pathophysiology and treatment,” *The Lancet Neurology*, vol. 8, no. 5, pp. 464–474, May 2009, doi: 10.1016/S1474-4422(09)70068-7.

[4] R. B. Postuma *et al.*, “MDS clinical diagnostic criteria for Parkinson’s disease,” *Movement Disorders*, vol. 30, no. 12, pp. 1591–1601, 2015, doi: 10.1002/mds.26424.

[5] G. Rizzo, M. Copetti, S. Arcuti, D. Martino, A. Fontana, and G. Logroscino, “Accuracy of clinical diagnosis of Parkinson disease: A systematic review and meta-analysis,” *Neurology*, vol. 86, no. 6, pp. 566–576, Feb. 2016, doi: 10.1212/WNL.0000000000002350.

[6] P. Damier, E. C. Hirsch, Y. Agid, and A. M. Graybiel, “The substantia nigra of the human brain: II. Patterns of loss of dopamine-containing neurons in Parkinson’s disease,” *Brain*, vol. 122, no. 8, pp. 1437–1448, Aug. 1999, doi: 10.1093/brain/122.8.1437.

[7] M. G. Spillantini, R. A. Crowther, R. Jakes, M. Hasegawa, and M. Goedert, “α-Synuclein in filamentous inclusions of Lewy bodies from Parkinson’s disease and dementia with Lewy bodies,” *PNAS*, vol. 95, no. 11, pp. 6469–6473, May 1998, doi: 10.1073/pnas.95.11.6469.

[8] D. W. Dickson *et al.*, “Neuropathological assessment of Parkinson’s disease: refining the diagnostic criteria,” *The Lancet Neurology*, vol. 8, no. 12, pp. 1150–1157, Dec. 2009, doi: 10.1016/S1474-4422(09)70238-8.

[9] T. J. Montine *et al.*, “National Institute on Aging–Alzheimer’s Association guidelines for the neuropathologic assessment of Alzheimer’s disease: a practical approach,” *Acta Neuropathol*, vol. 123, no. 1, pp. 1–11, Jan. 2012, doi: 10.1007/s00401-011-0910-3.

[10] W. Poewe *et al.*, “Parkinson disease,” *Nat Rev Dis Primers*, vol. 3, no. 1, p. 17013, Dec. 2017, doi: 10.1038/nrdp.2017.13.

[11] M. A. Nalls *et al.*, “Large-scale meta-analysis of genome-wide association data identifies six new risk loci for Parkinson’s disease,” *Nat Genet*, vol. 46, no. 9, pp. 989–993, Sep. 2014, doi: 10.1038/ng.3043.

[12] I. C. Brás, M. Xylaki, and T. F. Outeiro, “Chapter 4 - Mechanisms of alpha-synuclein toxicity: An update and outlook,” in *Progress in Brain Research*, vol. 252, A. Björklund and M. A. Cenci, Eds. Elsevier, 2020, pp. 91–129. doi: 10.1016/bs.pbr.2019.10.005.

[13] W. Springer and P. J. Kahle, “Mechanisms and models of α-

synuclein-related neurodegeneration," *Curr Neurol Neurosci Rep*, vol. 6, no. 5, pp. 432–436, Jan. 2006, doi: 10.1007/s11910-996-0025-8.
[14] A. Iwai *et al.*, "The precursor protein of non-Aβ component of Alzheimer's disease amyloid is a presynaptic protein of the central nervous system," *Neuron*, vol. 14, no. 2, pp. 467–475, Feb. 1995, doi: 10.1016/0896-6273(95)90302-X.
[15] J. T. Bendor, T. P. Logan, and R. H. Edwards, "The Function of α-Synuclein," *Neuron*, vol. 79, no. 6, pp. 1044–1066, Sep. 2013, doi: 10.1016/j.neuron.2013.09.004.
[16] J. Burré, "The Synaptic Function of α-Synuclein," *Journal of Parkinson's Disease*, vol. 5, no. 4, pp. 699–713, Jan. 2015, doi: 10.3233/JPD-150642.
[17] P. Garcia-Reitböck *et al.*, "SNARE protein redistribution and synaptic failure in a transgenic mouse model of Parkinson's disease," *Brain*, vol. 133, no. 7, pp. 2032–2044, Jul. 2010, doi: 10.1093/brain/awq132.
[18] S. Chandra, G. Gallardo, R. Fernández-Chacón, O. M. Schlüter, and T. C. Südhof, "α-Synuclein Cooperates with CSPα in Preventing Neurodegeneration," *Cell*, vol. 123, no. 3, pp. 383–396, Nov. 2005, doi: 10.1016/j.cell.2005.09.028.
[19] T. Bartels *et al.*, "The N-Terminus of the Intrinsically Disordered Protein α-Synuclein Triggers Membrane Binding and Helix Folding," *Biophys J*, vol. 99, no. 7, pp. 2116–2124, Oct. 2010, doi: 10.1016/j.bpj.2010.06.035.
[20] D. Eliezer, E. Kutluay, R. Bussell, and G. Browne, "Conformational properties of α-synuclein in its free and lipid-associated states11Edited by P. E. Wright," *Journal of Molecular Biology*, vol. 307, no. 4, pp. 1061–1073, Apr. 2001, doi: 10.1006/jmbi.2001.4538.
[21] T. S. Ulmer, A. Bax, N. B. Cole, and R. L. Nussbaum, "Structure and Dynamics of Micelle-bound Human α-Synuclein*," *Journal of Biological Chemistry*, vol. 280, no. 10, pp. 9595–9603, Mar. 2005, doi: 10.1074/jbc.M411805200.
[22] M. Bisaglia, I. Tessari, S. Mammi, and L. Bubacco, "Interaction Between α-Synuclein and Metal Ions, Still Looking for a Role in the Pathogenesis of Parkinson's Disease," *Neuromol Med*, vol. 11, no. 4, pp. 239–251, Dec. 2009, doi: 10.1007/s12017-009-8082-1.
[23] B. I. Giasson, I. V. Murray, J. Q. Trojanowski, and V. M. Lee, "A hydrophobic stretch of 12 amino acid residues in the middle of alpha-synuclein is essential for filament assembly," *J. Biol. Chem.*, vol. 276, no. 4, pp. 2380–2386, Jan. 2001, doi: 10.1074/jbc.M008919200.
[24] K. C. Luk *et al.*, "Exogenous α-synuclein fibrils seed the formation of Lewy body-like intracellular inclusions in cultured cells," *PNAS*, vol. 106, no. 47, pp. 20051–20056, Nov. 2009, doi: 10.1073/pnas.0908005106.
[25] H. Fujiwara *et al.*, "α-Synuclein is phosphorylated in synucleinopathy lesions," *Nat Cell Biol*, vol. 4, no. 2, pp. 160–164, Feb. 2002, doi: 10.1038/ncb748.
[26] A. Oueslati, M. Fournier, and H. A. Lashuel, "Chapter 7 - Role of post-translational modifications in modulating the structure, function and toxicity of α-synuclein: Implications for Parkinson's disease pathogenesis

and therapies," in *Progress in Brain Research*, vol. 183, A. Björklund and M. A. Cenci, Eds. Elsevier, 2010, pp. 115–145. doi: 10.1016/S0079-6123(10)83007-9.
[27] Y. Xu, Y. Deng, and H. Qing, "The phosphorylation of α-synuclein: development and implication for the mechanism and therapy of the Parkinson's disease," *Journal of Neurochemistry*, vol. 135, no. 1, pp. 4–18, 2015, doi: 10.1111/jnc.13234.
[28] S. Tenreiro, K. Eckermann, and T. F. Outeiro, "Protein phosphorylation in neurodegeneration: friend or foe?," *Front Mol Neurosci*, vol. 7, p. 42, May 2014, doi: 10.3389/fnmol.2014.00042.
[29] B. I. Giasson *et al.*, "Oxidative Damage Linked to Neurodegeneration by Selective α-Synuclein Nitration in Synucleinopathy Lesions," *Science*, vol. 290, no. 5493, pp. 985–989, Nov. 2000, doi: 10.1126/science.290.5493.985.
[30] R. Burai, N. Ait-Bouziad, A. Chiki, and H. A. Lashuel, "Elucidating the Role of Site-Specific Nitration of α-Synuclein in the Pathogenesis of Parkinson's Disease via Protein Semisynthesis and Mutagenesis," *J. Am. Chem. Soc.*, vol. 137, no. 15, pp. 5041–5052, Apr. 2015, doi: 10.1021/ja5131726.
[31] R. Hodara *et al.*, "Functional Consequences of α-Synuclein Tyrosine Nitration: DIMINISHED BINDING TO LIPID VESICLES AND INCREASED FIBRIL FORMATION *," *Journal of Biological Chemistry*, vol. 279, no. 46, pp. 47746–47753, Nov. 2004, doi: 10.1074/jbc.M408906200.
[32] J. P. Anderson *et al.*, "Phosphorylation of Ser-129 Is the Dominant Pathological Modification of α-Synuclein in Familial and Sporadic Lewy Body Disease*," *Journal of Biological Chemistry*, vol. 281, no. 40, pp. 29739–29752, Oct. 2006, doi: 10.1074/jbc.M600933200.
[33] J. Zhang, X. Li, and J.-D. Li, "The Roles of Post-translational Modifications on α-Synuclein in the Pathogenesis of Parkinson's Diseases," *Frontiers in Neuroscience*, vol. 13, p. 381, 2019, doi: 10.3389/fnins.2019.00381.
[34] C.-W. Liu, B. I. Giasson, K. A. Lewis, V. M. Lee, G. N. DeMartino, and P. J. Thomas, "A Precipitating Role for Truncated α-Synuclein and the Proteasome in α-Synuclein Aggregation: IMPLICATIONS FOR PATHOGENESIS OF PARKINSON DISEASE*," *Journal of Biological Chemistry*, vol. 280, no. 24, pp. 22670–22678, Jun. 2005, doi: 10.1074/jbc.M501508200.
[35] W. Li *et al.*, "Aggregation promoting C-terminal truncation of α-synuclein is a normal cellular process and is enhanced by the familial Parkinson's disease-linked mutations," *PNAS*, vol. 102, no. 6, pp. 2162–2167, Feb. 2005, doi: 10.1073/pnas.0406976102.
[36] W. Hoyer, D. Cherny, V. Subramaniam, and T. M. Jovin, "Impact of the Acidic C-Terminal Region Comprising Amino Acids 109–140 on α-Synuclein Aggregation in Vitro," *Biochemistry*, vol. 43, no. 51, pp. 16233–16242, Dec. 2004, doi: 10.1021/bi048453u.
[37] R. Melki, "Role of Different Alpha-Synuclein Strains in Synucleinopathies, Similarities with other Neurodegenerative Diseases," *J Parkinsons Dis*, vol. 5, no. 2, pp. 217–227, doi: 10.3233/JPD-150543.

[38] B. C. Jung *et al.*, “Amplification of distinct α-synuclein fibril conformers through protein misfolding cyclic amplification,” *Experimental & Molecular Medicine*, vol. 49, no. 4, Art. no. 4, Apr. 2017, doi: 10.1038/emm.2017.1.
[39] H. LeVine, “Thioflavine T interaction with synthetic Alzheimer’s disease beta-amyloid peptides: detection of amyloid aggregation in solution.,” *Protein Sci*, vol. 2, no. 3, pp. 404–410, Mar. 1993.
[40] H. PUCHTLER and F. SWEAT, “CONGO RED AS A STAIN FOR FLUORESCENCE MICROSCOPY OF AMYLOID,” *J Histochem Cytochem.*, vol. 13, no. 8, pp. 693–694, Nov. 1965, doi: 10.1177/13.8.693.
[41] D. W. Dickson *et al.*, “Diffuse Lewy body disease: light and electron microscopic immunocytochemistry of senile plaques,” *Acta Neuropathol*, vol. 78, no. 6, pp. 572–584, Nov. 1989, doi: 10.1007/BF00691284.
[42] P. J. Kahle *et al.*, “Selective Insolubility of α-Synuclein in Human Lewy Body Diseases Is Recapitulated in a Transgenic Mouse Model,” *The American Journal of Pathology*, vol. 159, no. 6, pp. 2215–2225, Dec. 2001, doi: 10.1016/S0002-9440(10)63072-6.
[43] P. J. Kahle *et al.*, “Subcellular Localization of Wild-Type and Parkinson’s Disease-Associated Mutant α-Synuclein in Human and Transgenic Mouse Brain,” *J. Neurosci.*, vol. 20, no. 17, pp. 6365–6373, Sep. 2000, doi: 10.1523/JNEUROSCI.20-17-06365.2000.
[44] H. A. Lashuel, C. R. Overk, A. Oueslati, and E. Masliah, “The many faces of α-synuclein: from structure and toxicity to therapeutic target,” *Nature Reviews Neuroscience*, vol. 14, no. 1, Art. no. 1, Jan. 2013, doi: 10.1038/nrn3406.
[45] W. Paslawski, N. Lorenzen, and D. E. Otzen, “Formation and Characterization of α-Synuclein Oligomers,” in *Protein Amyloid Aggregation: Methods and Protocols*, D. Eliezer, Ed. New York, NY: Springer, 2016, pp. 133–150. doi: 10.1007/978-1-4939-2978-8_9.
[46] V. N. Uversky, J. Li, and A. L. Fink, “Metal-triggered Structural Transformations, Aggregation, and Fibrillation of Human α-Synuclein: A POSSIBLE MOLECULAR LINK BETWEEN PARKINSON'S DISEASE AND HEAVY METAL EXPOSURE*,” *Journal of Biological Chemistry*, vol. 276, no. 47, pp. 44284–44296, Nov. 2001, doi: 10.1074/jbc.M105343200.
[47] J. M. Souza, B. I. Giasson, Q. Chen, V. M.-Y. Lee, and H. Ischiropoulos, “Dityrosine Cross-linking Promotes Formation of Stable α-Synuclein Polymers: IMPLICATION OF NITRATIVE AND OXIDATIVE STRESS IN THE PATHOGENESIS OF NEURODEGENERATIVE SYNUCLEINOPATHIES *,” *Journal of Biological Chemistry*, vol. 275, no. 24, pp. 18344–18349, Jun. 2000, doi: 10.1074/jbc.M000206200.
[48] K. A. Conway, J.-C. Rochet, R. M. Bieganski, and P. T. Lansbury, “Kinetic Stabilization of the α-Synuclein Protofibril by a Dopamine-α-Synuclein Adduct,” *Science*, vol. 294, no. 5545, pp. 1346–1349, Nov. 2001, doi: 10.1126/science.1063522.
[49] W. Paslawski *et al.*, “High Stability and Cooperative Unfolding of α-Synuclein Oligomers,” *Biochemistry*, vol. 53, no. 39, pp. 6252–6263, Oct. 2014, doi: 10.1021/bi5007833.
[50] P. Alam, L. Bousset, R. Melki, and D. E. Otzen, “α-synuclein

oligomers and fibrils: a spectrum of species, a spectrum of toxicities," *Journal of Neurochemistry*, vol. 150, no. 5, pp. 522–534, 2019, doi: 10.1111/jnc.14808.
[51] W. P. Flavin *et al.*, "Endocytic vesicle rupture is a conserved mechanism of cellular invasion by amyloid proteins," *Acta Neuropathol*, vol. 134, no. 4, pp. 629–653, Oct. 2017, doi: 10.1007/s00401-017-1722-x.
[52] R. I. Morimoto, "The Heat Shock Response: Systems Biology of Proteotoxic Stress in Aging and Disease," *Cold Spring Harb Symp Quant Biol*, vol. 76, pp. 91–99, Jan. 2011, doi: 10.1101/sqb.2012.76.010637.
[53] A. Hoffmann *et al.*, "Alpha-synuclein activates BV2 microglia dependent on its aggregation state," *Biochemical and Biophysical Research Communications*, vol. 479, no. 4, pp. 881–886, Oct. 2016, doi: 10.1016/j.bbrc.2016.09.109.
[54] L. Bousset *et al.*, "Structural and functional characterization of two alpha-synuclein strains," *Nature Communications*, vol. 4, no. 1, Art. no. 1, Oct. 2013, doi: 10.1038/ncomms3575.
[55] M. X. Henderson, J. Q. Trojanowski, and V. M.-Y. Lee, "α-Synuclein pathology in Parkinson's disease and related α-synucleinopathies," *Neuroscience Letters*, vol. 709, p. 134316, Sep. 2019, doi: 10.1016/j.neulet.2019.134316.
[56] W. J. Schulz-Schaeffer, "The synaptic pathology of α-synuclein aggregation in dementia with Lewy bodies, Parkinson's disease and Parkinson's disease dementia," *Acta Neuropathol*, vol. 120, no. 2, pp. 131–143, Aug. 2010, doi: 10.1007/s00401-010-0711-0.
[57] A. Bellucci, L. Navarria, M. Zaltieri, C. Missale, and P. Spano, "Alpha-synuclein synaptic pathology and its implications in the development of novel therapeutic approaches to cure Parkinson's disease," *Brain Research*, vol. 1432, pp. 95–113, Jan. 2012, doi: 10.1016/j.brainres.2011.11.031.
[58] K. M. Danzer *et al.*, "Different Species of α-Synuclein Oligomers Induce Calcium Influx and Seeding," *J. Neurosci.*, vol. 27, no. 34, pp. 9220–9232, Aug. 2007, doi: 10.1523/JNEUROSCI.2617-07.2007.
[59] L. M. Chahine *et al.*, "In vivo distribution of α-synuclein in multiple tissues and biofluids in Parkinson disease," *Neurology*, vol. 95, no. 9, pp. e1267–e1284, Sep. 2020, doi: 10.1212/WNL.0000000000010404.
[60] L. Parnetti *et al.*, "CSF and blood biomarkers for Parkinson's disease," *The Lancet Neurology*, vol. 18, no. 6, pp. 573–586, Jun. 2019, doi: 10.1016/S1474-4422(19)30024-9.
[61] S. M. Williams, P. Schulz, and M. R. Sierks, "Oligomeric α-synuclein and β-amyloid variants as potential biomarkers for Parkinson's and Alzheimer's diseases," *European Journal of Neuroscience*, vol. 43, no. 1, pp. 3–16, 2016, doi: 10.1111/ejn.13056.
[62] P. G. Foulds *et al.*, "Phosphorylated α-synuclein can be detected in blood plasma and is potentially a useful biomarker for Parkinson's disease," *FASEB j.*, vol. 25, no. 12, pp. 4127–4137, Dec. 2011, doi: 10.1096/fj.10-179192.
[63] M. Shi *et al.*, "Significance and confounders of peripheral DJ-1 and alpha-synuclein in Parkinson's disease," *Neuroscience Letters*, vol. 480, no.

1, pp. 78–82, Aug. 2010, doi: 10.1016/j.neulet.2010.06.009.
[64] R. Barbour *et al.*, “Red Blood Cells Are the Major Source of Alpha-Synuclein in Blood,” *NDD*, vol. 5, no. 2, pp. 55–59, 2008, doi: 10.1159/000112832.
[65] M. Rossi *et al.*, “Ultrasensitive RT-QuIC assay with high sensitivity and specificity for Lewy body-associated synucleinopathies,” *Acta Neuropathol*, vol. 140, no. 1, pp. 49–62, Jul. 2020, doi: 10.1007/s00401-020-02160-8.
[66] M. Shahnawaz *et al.*, “Development of a Biochemical Diagnosis of Parkinson Disease by Detection of α-Synuclein Misfolded Aggregates in Cerebrospinal Fluid,” *JAMA Neurology*, vol. 74, no. 2, pp. 163–172, Feb. 2017, doi: 10.1001/jamaneurol.2016.4547.
[67] T. Strohäker *et al.*, “Structural heterogeneity of α-synuclein fibrils amplified from patient brain extracts,” *Nat Commun*, vol. 10, no. 1, p. 5535, Dec. 2019, doi: 10.1038/s41467-019-13564-w.
[68] C. Peng *et al.*, “Cellular milieu imparts distinct pathological α-synuclein strains in α-synucleinopathies,” *Nature*, vol. 557, no. 7706, pp. 558–563, May 2018, doi: 10.1038/s41586-018-0104-4.
[69] S. T. Kumar, S. Donzelli, A. Chiki, M. M. K. Syed, and H. A. Lashuel, “A simple, versatile and robust centrifugation-based filtration protocol for the isolation and quantification of α-synuclein monomers, oligomers and fibrils: Towards improving experimental reproducibility in α-synuclein research,” *J. Neurochem.*, vol. 153, no. 1, pp. 103–119, Apr. 2020, doi: 10.1111/jnc.14955.
[70] B. Fauvet *et al.*, “α-Synuclein in Central Nervous System and from Erythrocytes, Mammalian Cells, and Escherichia coli Exists Predominantly as Disordered Monomer,” *J. Biol. Chem.*, vol. 287, no. 19, pp. 15345–15364, May 2012, doi: 10.1074/jbc.M111.318949.
[71] S. T. Kumar, S. Jagannath, C. Francois, H. Vanderstichele, E. Stoops, and H. A. Lashuel, “How specific are the conformation-specific α-synuclein antibodies? Characterization and validation of 16 α-synuclein conformation-specific antibodies using well-characterized preparations of α-synuclein monomers, fibrils and oligomers with distinct structures and morphology,” *Neurobiology of Disease*, vol. 146, p. 105086, Dec. 2020, doi: 10.1016/j.nbd.2020.105086.
[72] H.-J. Lee, S. Y. Shin, C. Choi, Y. H. Lee, and S.-J. Lee, “Formation and Removal of α-Synuclein Aggregates in Cells Exposed to Mitochondrial Inhibitors*,” *Journal of Biological Chemistry*, vol. 277, no. 7, pp. 5411–5417, Feb. 2002, doi: 10.1074/jbc.M105326200.
[73] T. Ikenoue *et al.*, “Cold Denaturation of α-Synuclein Amyloid Fibrils,” *Angewandte Chemie International Edition*, vol. 53, no. 30, pp. 7799–7804, 2014, doi: https://doi.org/10.1002/anie.201403815.
[74] H.-J. Lee *et al.*, “Enzyme-linked immunosorbent assays for alpha-synuclein with species and multimeric state specificities,” *Journal of Neuroscience Methods*, vol. 199, no. 2, pp. 249–257, Aug. 2011, doi: 10.1016/j.jneumeth.2011.05.020.
[75] N. Lorenzen *et al.*, “The Role of Stable α-Synuclein Oligomers in the Molecular Events Underlying Amyloid Formation,” *J. Am. Chem. Soc.*,

vol. 136, no. 10, pp. 3859–3868, Mar. 2014, doi: 10.1021/ja411577t.
[76] C. S. McAlpine *et al.*, "Astrocytic interleukin-3 programs microglia and limits Alzheimer's disease," *Nature*, pp. 1–6, Jul. 2021, doi: 10.1038/s41586-021-03734-6.
[77] S. D. Schmidt, R. A. Nixon, and P. M. Mathews, "ELISA Method for Measurement of Amyloid-ß Levels," in *Amyloid Proteins: Methods and Protocols*, E. M. Sigurdsson, Ed. Totowa, NJ: Humana Press, 2005, pp. 279–297. doi: 10.1385/1-59259-874-9:279.
[78] M. G. Spillantini, M. L. Schmidt, V. M.-Y. Lee, J. Q. Trojanowski, R. Jakes, and M. Goedert, "α-Synuclein in Lewy bodies," *Nature*, vol. 388, no. 6645, pp. 839–840, Aug. 1997, doi: 10.1038/42166.
[79] K. C. Luk *et al.*, "Pathological α-Synuclein Transmission Initiates Parkinson-like Neurodegeneration in Nontransgenic Mice," *Science*, vol. 338, no. 6109, pp. 949–953, Nov. 2012, doi: 10.1126/science.1227157.
[80] L. A. Volpicelli-Daley *et al.*, "Exogenous α-Synuclein Fibrils Induce Lewy Body Pathology Leading to Synaptic Dysfunction and Neuron Death," *Neuron*, vol. 72, no. 1, pp. 57–71, Oct. 2011, doi: 10.1016/j.neuron.2011.08.033.
[81] G. P. Saborio, B. Permanne, and C. Soto, "Sensitive detection of pathological prion protein by cyclic amplification of protein misfolding," *Nature*, vol. 411, no. 6839, pp. 810–813, Jun. 2001, doi: 10.1038/35081095.
[82] Y. Kim *et al.*, "Comparative analyses of plasma amyloid-β levels in heterogeneous and monomerized states by interdigitated microelectrode sensor system," *Science Advances*, vol. 5, no. 4, p. eaav1388, Apr. 2019, doi: 10.1126/sciadv.aav1388.
[83] Y. C. Youn *et al.*, "Blood Amyloid-β Oligomerization as a Biomarker of Alzheimer's Disease: A Blinded Validation Study," *Journal of Alzheimer's Disease*, vol. 75, no. 2, pp. 493–499, Jan. 2020, doi: 10.3233/JAD-200061.
[84] R. Chandra, A. Hiniker, Y.-M. Kuo, R. L. Nussbaum, and R. A. Liddle, "α-Synuclein in gut endocrine cells and its implications for Parkinson's disease," *JCI Insight*, vol. 2, no. 12, p. e92295, doi: 10.1172/jci.insight.92295.
[85] M. Shi *et al.*, "Plasma exosomal α-synuclein is likely CNS-derived and increased in Parkinson's disease," *Acta Neuropathol*, vol. 128, no. 5, pp. 639–650, Nov. 2014, doi: 10.1007/s00401-014-1314-y.
[86] M. Niu *et al.*, "A longitudinal study on α-synuclein in plasma neuronal exosomes as a biomarker for Parkinson's disease development and progression," *European Journal of Neurology*, vol. 27, no. 6, pp. 967–974, 2020, doi: https://doi.org/10.1111/ene.14208.
[87] M. Norman *et al.*, "L1CAM is not associated with extracellular vesicles in human cerebrospinal fluid or plasma," *Nat Methods*, vol. 18, no. 6, pp. 631–634, Jun. 2021, doi: 10.1038/s41592-021-01174-8.
[88] Y.-T. Sui, K. M. Bullock, M. A. Erickson, J. Zhang, and W. A. Banks, "Alpha synuclein is transported into and out of the brain by the blood–brain barrier," *Peptides*, vol. 62, pp. 197–202, Dec. 2014, doi: 10.1016/j.peptides.2014.09.018.
[89] J. Matsumoto *et al.*, "Transmission of α-synuclein-containing erythrocyte-derived extracellular vesicles across the blood-brain barrier via adsorptive mediated transcytosis: another mechanism for initiation and

progression of Parkinson's disease?," *Acta Neuropathologica Communications*, vol. 5, no. 1, p. 71, Sep. 2017, doi: 10.1186/s40478-017-0470-4.

국문 초록

파킨슨병은 진행되는 퇴행성 뇌질환으로 병리학적 소견으로는 알파 시뉴클린 축적과 흑질에서의 선택적인 도파민 생성 뉴런의 손실이 관찰된다. 알파 시뉴클린 피브릴은 루이체와 루이신경돌기의 주요 구성성분이다. 이러한 알파 시뉴클린 응집체는 다양한 세포 경로를 통해 뉴런 기능의 손실과 사멸을 가져오는 것으로 알려져 있다. 또한, 응집체는 세포간 전파가 가능하여 시간이 지나면서 뇌에 더 광범위하게 퍼져 병이 더욱 악화된다. 알파 시뉴클린이 파킨슨병의 병태생리에 중요한 역할을 하기에 알파 시뉴클린을 혈액과 뇌척수액에서 측정하여 바이오마커로 이용하고자 하는 다양한 시도가 있었다. 그렇지만 알파 시뉴클린 피브릴을 혈액에서 검출하거나 비교한 연구는 지금까지 없었다. 따라서, 본 연구는 알파 시뉴클린 피브릴이 일반적으로 사람의 혈장에 존재를 하는지 규명하고자 하였다. 최근에 발표된 논문을 바탕으로 하여 측정 방법을 새로 수립하였으며 이를 통해 재조합 알파 시뉴클린 단백질을 크기에 따라 (monomer, oligomer, fibril) 구분하여 측정할 수 있음을 보였다. 더 나아가 혈액에서 동일한 방법을 적용하여 피브릴 크기의 고분자 응집체를 검출할 수 있음을 보였다. 이와 같은 결과는 혈장내 알파 시뉴클린 피브릴의 정량적, 정성적 비교를 통한 새로운 파킨슨병 진단법 개발의 가능성을 보여준다.

주제어 : 신경퇴행성질환, 파킨슨병, 알파 시뉴클린, 아밀로이드 피브릴, 혈장, ELISA

학번 : 2020-22060